



Centrum voor Wiskunde en Informatica

**REPORT**RAPPORT

**MAS**

Modelling, Analysis and Simulation



*Modelling, Analysis and Simulation*

On a two-dimensional discontinuous Galerkin  
discretisation with embedded Dirichlet boundary condition

M.H. van Raalte

**REPORT MAS-R0306 JULY 31, 2003**

CWI is the National Research Institute for Mathematics and Computer Science. It is sponsored by the Netherlands Organization for Scientific Research (NWO).

CWI is a founding member of ERCIM, the European Research Consortium for Informatics and Mathematics.

CWI's research has a theme-oriented structure and is grouped into four clusters. Listed below are the names of the clusters and in parentheses their acronyms.

Probability, Networks and Algorithms (PNA)

Software Engineering (SEN)

Modelling, Analysis and Simulation (MAS)

Information Systems (INS)

Copyright © 2003, Stichting Centrum voor Wiskunde en Informatica  
P.O. Box 94079, 1090 GB Amsterdam (NL)  
Kruislaan 413, 1098 SJ Amsterdam (NL)  
Telephone +31 20 592 9333  
Telefax +31 20 592 4199

ISSN 1386-3711

# On a two-dimensional Discontinuous Galerkin Discretisation with embedded Dirichlet boundary condition

M.H. van Raalte

*KdV Institute for Mathematics, University of Amsterdam*

*Plantage Muidergracht 24, 1018 TV Amsterdam, The Netherlands*

CWI

*P.O. Box 94079, 1090 GB Amsterdam, The Netherlands*

## ABSTRACT

In this paper we introduce a discretisation of Discontinuous Galerkin (DG) type for solving 2-D second order elliptic PDEs on a regular rectangular grid, while the boundary value problem has a curved Dirichlet boundary. According to the same principles that underlie DG-methods, we adapt the discretisation in the cell in which the (embedded) Dirichlet boundary cannot follow the gridlines of the orthogonal grid.

The DG-discretisation aims at a high order of accuracy. We discretize with tensor products of cubic polynomials. By construction, such a DG discretisation is fourth order consistent, both in the interior and at the boundaries. By experiments we show fourth order convergence in the presence of a curved Dirichlet boundary. Stability is proved for the one-dimensional Poisson equation with an embedded boundary condition.

To illustrate the possibilities of our DG-discretisation, we solve a convection dominated boundary value problem on a regular rectangular grid with a circular embedded boundary condition [7]. We show how accurately the boundary layer with a complex structure can be captured by means of piece-wise cubic polynomials. The example shows that the embedded boundary treatment is effective.

*2000 Mathematics Subject Classification:* 65N50, 65N99

*Keywords and Phrases:* Discontinuous Galerkin (DG) methods, structured grid, embedded boundary

## 1. INTRODUCTION

In this paper we introduce a new discontinuous Galerkin (DG) technique using a regular grid for solving two-dimensional elliptic boundary value problems on complex domains. So the difficulty arises that a part of the boundary (the embedded boundary) cannot follow the gridlines.

Since renewed insights into discontinuous Galerkin methods for elliptic PDEs were obtained, [14, 4, 1, 18], these methods gain in popularity. Especially, because of their convenient properties when combined with the *hp*-adaptive approach and multi-grid solvers [19, 12, 20, 10].

In view of such applications we want to solve elliptic PDEs with a DG-method on a regular rectangular grid, while the embedded boundary is typically not aligned with the grid, but rather intersects the edges of the grid. The main advantage of such a DG-method for the

embedded boundary is the efficient and easy grid generation compared to the unstructured grid methods. Even moving-boundary problems could be handled with this DG-method for the embedded boundary without regenerating grids in time.

The most classical technique in treating complex boundaries is certainly the FEM, where elements near the boundary are adapted to the shape of the boundary curve. This method is convenient for high order discretisations. However, generally, the advantages of having a structured grid is lost.

In the field of finite difference methods, the finite differences are locally adapted to the curved boundary while the total domain is a regular structured grid. A recent example is the Embedded Curved Boundary (ECB) Method for higher dimensions, in which the curved boundary is approximated by piecewise linear segments [11, 13]. This method is fast and has all the advantages of having a regular structured grid, however no order of accuracy can be expected higher than two.

Another method which treats complex geometries on orthogonal meshes, is the immersed boundary (IB) method. This method was previously introduced by Peskin [17, 21] as a method to study biofluid dynamics problems. Examples of applications are the coupled motion of the blood filling the verticles of the hart and the interaction between flexible elastic membranes in combination with an incompressible fluid in two dimensions [6]. The main idea of this method is to introduce a body force term such that the presence of the embedded boundary is simulated, without altering the orthogonal mesh. This approach makes the method very flexible and even fourth order convergences is reported [6].

Our approach is to introduce a domain  $\hat{\Omega}$  slightly larger than the domain  $\Omega$  on which the BVP is originally defined. Then, according to the typical DG setting, we treat the embedded boundary in weak form, by introducing a Lagrange multiplier, assuming that the solution on the fictitious domain has a sufficiently smooth continuation satisfying the PDE on the whole of  $\hat{\Omega}$ . Of course, this will imply to the requirement that the local domains  $\Omega_e$  of cells  $\hat{\Omega}_e$ , do not vanish.

Applying this Lagrange-multiplier technique, we arrive at two main formulations: the *Lagrange formulation* for the embedded boundary condition, and the *hybrid formulation* [9]. In Section 2, we give an exposure of these two formulations and study the stability conditions. From both forms DG-formulations for the embedded boundary can be derived by elimination of the Lagrange multiplier. We will see in Section 3 that these formulations are easily applied to BVP's on complex domains. However, depending on the location of the embedded boundary, stability is not always guaranteed. On the other hand this possible instability can be repaired. We prove that for the one-dimensional Poisson equation on a single cell, the Baumann-Oden variant is stable, if we only weight the embedded boundary with the traces of two linear polynomials. In Section 4 we introduce a DG-discretisation technique for solving the Poisson equation on a rectangular grid, while a part of the boundary, the embedded boundary, is curved. For test and trial space we take the cubic tensor product polynomials, the basis of higher-order approximations as explained in [8], and we show that such a discretisation technique is fourth-order consistent both in the interior and at the boundaries. By experiments, we show that on halving the gridsize an average error reduction of a factor 12 can be expected, if an extra weight is introduced, weighting the embedded boundary with the trace of a linear polynomial. Moreover, by introducing this weight, the corresponding linear systems become positive definite.

It is straight forward to extend the use of the DG-technique for the embedded boundary condition to the convection-diffusion equation. This is explained in Section 4.3. In the last Section we solve a singularly perturbed convection-dominated boundary value problem with an embedded circular boundary. We show how well the complex structure of the solution is captured by means of piecewise cubics.

Summarizing, we show that the proposed DG discretisation technique for the treatment of curved Dirichlet boundary conditions on a regular rectangular grid is effective.

## 2. LAGRANGE MULTIPLIER FORMS

### 2.1 The Lagrange multiplier form for the embedded boundary condition

In order to solve a second order elliptic problem  $Lu = f$  on a complex domain by means of a DG-discretisation type, we consider the equation on an open domain  $\widehat{\Omega}$ , which is slightly larger than the open domain  $\Omega$  on which the elliptic BVP is originally defined. On this fictitious domain  $\widehat{\Omega} \supseteq \Omega$  we discretize the problem  $Lu = f$ . The solution  $u$  is determined by a Dirichlet boundary condition  $u = u_0$  on  $\partial\Omega$ , the boundary of  $\Omega$ , and we assume that this solution  $u$  allows for a sufficiently smooth continuation on the whole of  $\widehat{\Omega}$ . Of course, this excludes certain types of singularities near the boundary.

For this treatment we consider a rectangular domain  $\widehat{\Omega}$  with boundary  $\partial\widehat{\Omega}$  as in Figure 1. In this domain we distinguish two non-overlapping open sub-domains,  $\Omega$  and  $\widetilde{\Omega}$ , such that

$$\overline{\widehat{\Omega}} = \overline{\Omega} \cup \overline{\widetilde{\Omega}}, \quad \text{and} \quad \Omega \cap \widetilde{\Omega} = \emptyset, \quad (2.1)$$

where  $\Omega$  is the domain of interest and  $\widetilde{\Omega}$  is the fictitious part. On the whole domain  $\widehat{\Omega}$ , we now apply the differential equation, while the Dirichlet boundary conditions are given on  $\partial\Omega$ , the boundary of  $\Omega$ . So, for the Poisson equation our boundary value problem reads:

$$Lu \equiv -\Delta u = f \quad \text{on } \widehat{\Omega}, \quad \text{and} \quad u = u_0 \quad \text{on } \Gamma_D = \partial\Omega, \quad (2.2)$$

under the assumption that the solution  $u$  on  $\Omega$ , has a sufficiently smooth continuation into  $\widetilde{\Omega}$ , satisfying the Poisson equation on the whole of  $\widehat{\Omega}$ .

To arrive at a mesh-dependent variational formulation of the Poisson equation, we consider a partitioning,  $\widehat{\Omega}_h$ , of  $\widehat{\Omega}$  in regular rectangular cells, such that

$$\widehat{\Omega}_h = \left\{ \widehat{\Omega}_e \mid \cup_e \widehat{\Omega}_e = \widehat{\Omega}, \widehat{\Omega}_i \cap \widehat{\Omega}_j = \emptyset, i \neq j \right\}. \quad (2.3)$$

By the partitioning (2.3), we introduce the set of common interfaces between adjacent cells,  $\widehat{\Gamma}_{\text{int}} = \widehat{\Omega}_i \cap \widehat{\Omega}_j$ . In this way, cells  $\widehat{\Omega}_e$  which contain part of the embedded boundary  $\gamma_e \subset \partial\Omega$  are split into two coherent parts,  $\Omega_e = \widehat{\Omega}_e \cap \Omega$  and  $\widetilde{\Omega}_e = \widehat{\Omega}_e \cap \widetilde{\Omega}$  so that  $\widehat{\Gamma}_{\text{int}} = \Gamma_{\text{int}} \cap \widetilde{\Gamma}_{\text{int}}$ , where  $\Gamma_{\text{int}} = \overline{\Omega}_i \cap \overline{\Omega}_j$  is the interface not including the fictitious part, while the interface in the fictitious part of the domain is  $\widetilde{\Gamma}_{\text{int}} = \widetilde{\Omega}_i \cap \widetilde{\Omega}_j$ . (See also Figure 1.)

On the partitioning (2.3), we consider the broken Sobolev space [4, 16, 5] for non-negative integer  $k$ , defined by

$$H^k(\widehat{\Omega}_h) = \left\{ u \in L_2(\widehat{\Omega}) \mid u|_{\widehat{\Omega}_e} \in H^k(\widehat{\Omega}_e), \forall \widehat{\Omega}_e \in \widehat{\Omega}_h \right\}.$$

Now the weak formulation for the Poisson equation with an embedded Dirichlet boundary condition reads: find  $u \in H^1(\widehat{\Omega}_h)$  and  $p \in H^{-1/2}(\Gamma_{\text{int}})$  such that

$$\begin{aligned} & \sum_{\widehat{\Omega}_e \in \widehat{\Omega}_h} (\nabla u, \nabla v)_{\widehat{\Omega}_e} - \langle \nabla u, [v] \rangle_{\partial \widehat{\Omega}} - \langle p, [v] \rangle_{\Gamma_{\text{int}}} - \langle q, [u] \rangle_{\Gamma_{\text{int}}} \\ &= \sum_{\widehat{\Omega}_e \in \widehat{\Omega}_h} (f, v)_{\widehat{\Omega}_e}, \quad \forall v \in H^1(\widehat{\Omega}_h), \quad \forall q \in H^{-1/2}(\Gamma_{\text{int}}), \end{aligned} \quad (2.4)$$

under the constraint that  $u = u_0$  on  $\partial \Omega$ .

Here, we define the jump operator  $[\cdot]$  at the common interfaces  $\widehat{\Gamma}_{\text{int}}$  and  $\Gamma_{\text{int}}$  between two adjacent<sup>1</sup> cells  $\widehat{\Omega}_i$  and  $\widehat{\Omega}_j$  by

$$\begin{aligned} \widehat{\Gamma}_{\text{int}} : \quad [w(x)] &= w(x)|_{\partial \widehat{\Omega}_i} \mathbf{n}_i + w(x)|_{\partial \widehat{\Omega}_j} \mathbf{n}_j, \\ \Gamma_{\text{int}} : \quad [w(x)] &= w(x)|_{\partial \Omega_i} \mathbf{n}_i + w(x)|_{\partial \Omega_j} \mathbf{n}_j. \end{aligned} \quad (2.5)$$

Notice, that the term  $\langle q, [u] \rangle_{\Gamma_{\text{int}}}$  is also computed at interfaces of cells  $\widehat{\Omega}_e$  not containing part of the embedded boundary  $\gamma$ , since we then have  $\widetilde{\Gamma}_{\text{int}} = \emptyset$  and hence  $\widehat{\Gamma}_{\text{int}} = \Gamma_{\text{int}}$ . In this way, we only require continuity of the solution  $u$  in the domain of interest (see also [9], page 152).

For a vanishing fictitious part  $\widetilde{\Omega}$ , we recognize in (2.4) the classical hybrid formulation for the Poisson equation as described in [3, 15], but in this case with strongly imposed Dirichlet boundary conditions.

By the Lagrange multiplier theorem [2], (2.4) is equivalent to the following form: find  $u \in H^1(\widehat{\Omega}_h)$ ,  $p \in H^{-1/2}(\Gamma_{\text{int}})$  and  $\bar{p} \in H^{-1/2}(\partial \Omega)$  such that

$$\begin{aligned} & \sum_{\widehat{\Omega}_e \in \widehat{\Omega}_h} (\nabla u, \nabla v)_{\widehat{\Omega}_e} - \langle \nabla u, [v] \rangle_{\partial \widehat{\Omega}} + \langle \bar{p}, [v] \rangle_{\partial \Omega} - \langle p, [v] \rangle_{\Gamma_{\text{int}}} - \langle q, [u] \rangle_{\Gamma_{\text{int}}} \\ &= \sum_{\widehat{\Omega}_e \in \widehat{\Omega}_h} (f, v)_{\widehat{\Omega}_e}, \quad \forall v \in H^1(\widehat{\Omega}_h), \quad \forall q \in H^{-1/2}(\Gamma_{\text{int}}), \\ & \langle q, [u] \rangle_{\partial \Omega} = \langle q, [u_0] \rangle_{\partial \Omega} \quad \forall q \in H^{-1/2}(\partial \Omega). \end{aligned} \quad (2.6)$$

We call this form the general *Lagrange formulation* for the embedded boundary value problem (see also [9], page 137). We see that if  $u$  satisfies (2.2), that  $p$  satisfies  $p = \nabla u$  and  $\bar{p}$  vanishes at the boundary  $\partial \Omega$ .

## 2.2 The hybrid form for the embedded boundary condition

We also introduce an alternative formulation for the embedded boundary condition. For this purpose, we consider the general Lagrange formulation for the embedded boundary value problem (2.6). For vanishing fictitious part  $\widetilde{\Omega} = \emptyset$  of the domain  $\widehat{\Omega}$ , formulation (2.6) reads:

---

<sup>1</sup>At the boundaries  $\partial \widehat{\Omega}$  and  $\partial \Omega$  the interface with a virtual (flat, exterior) adjacent cell is used.

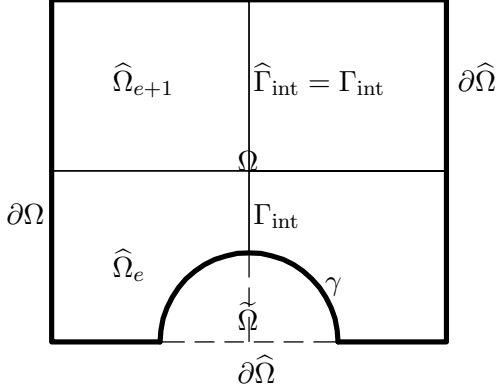


Figure 1: The partitioning  $\widehat{\Omega}_h$ , the domain of interest  $\Omega$  and the fictitious part  $\widehat{\Omega}$ . The fictitious domain  $\widehat{\Omega} = \Omega \cup \widehat{\Omega}$ .

find  $u \in H^1(\widehat{\Omega}_h)$ ,  $p \in H^{-1/2}(\widehat{\Gamma}_{\text{int}})$  and  $\bar{p} \in H^{-1/2}(\partial\widehat{\Omega})$  such that

$$\begin{aligned} & \sum_{\widehat{\Omega}_e \in \widehat{\Omega}_h} (\nabla u, \nabla v)_{\widehat{\Omega}_e} - \langle \nabla u, [v] \rangle_{\partial\widehat{\Omega}} + \langle \bar{p}, [v] \rangle_{\partial\widehat{\Omega}} - \langle p, [v] \rangle_{\widehat{\Gamma}_{\text{int}}} - \langle q, [u] \rangle_{\widehat{\Gamma}_{\text{int}}} \\ &= \sum_{\widehat{\Omega}_e \in \widehat{\Omega}_h} (f, v)_{\widehat{\Omega}_e}, \quad \forall v \in H^1(\widehat{\Omega}_h), \quad \forall q \in H^{-1/2}(\widehat{\Gamma}_{\text{int}}), \\ & \langle q, [u] \rangle_{\partial\widehat{\Omega}} = \langle q, [u_0] \rangle_{\partial\widehat{\Omega}} \quad \forall q \in H^{-1/2}(\partial\widehat{\Omega}). \end{aligned} \quad (2.7)$$

Taking  $p|_{\partial\widehat{\Omega}} = (\nabla u - \bar{p})|_{\partial\widehat{\Omega}}$ , we arrive at the classical hybrid weak formulation [3, 15]: find  $u \in H^1(\widehat{\Omega}_h)$ ,  $p \in H^{-1/2}(\widehat{\Gamma}_{\text{int}} \cup \partial\widehat{\Omega})$  such that

$$\begin{aligned} & \sum_{\widehat{\Omega}_e \in \widehat{\Omega}_h} (\nabla u, \nabla v)_{\widehat{\Omega}_e} - \langle p, [v] \rangle_{\partial\widehat{\Omega}} - \langle q, [u] \rangle_{\partial\widehat{\Omega}} - \langle p, [v] \rangle_{\widehat{\Gamma}_{\text{int}}} - \langle q, [u] \rangle_{\widehat{\Gamma}_{\text{int}}} \\ &= \sum_{\widehat{\Omega}_e \in \widehat{\Omega}_h} (f, v)_{\widehat{\Omega}_e} - \langle q, [u_0] \rangle_{\partial\widehat{\Omega}}, \quad \forall v \in H^1(\widehat{\Omega}_h), \quad \forall q \in H^{-1/2}(\widehat{\Gamma}_{\text{int}} \cup \partial\widehat{\Omega}). \end{aligned} \quad (2.8)$$

However, we can also apply (2.8) to the embedded boundary value problem. Then, in case of  $\widehat{\Omega} \neq \emptyset$ , the weak formulation reads: find  $u \in H^1(\widehat{\Omega}_h)$ ,  $p \in H^{-1/2}(\widehat{\Gamma}_{\text{int}} \cup \partial\widehat{\Omega})$  such that

$$\begin{aligned} & \sum_{\widehat{\Omega}_e \in \widehat{\Omega}_h} (\nabla u, \nabla v)_{\widehat{\Omega}_e} - \langle p, [v] \rangle_{\partial\widehat{\Omega}} - \langle q, [u] \rangle_{\partial\Omega} - \langle p, [v] \rangle_{\widehat{\Gamma}_{\text{int}}} - \langle q, [u] \rangle_{\Gamma_{\text{int}}} \\ &= \sum_{\widehat{\Omega}_e \in \widehat{\Omega}_h} (f, v)_{\widehat{\Omega}_e} - \langle q, [u_0] \rangle_{\partial\Omega}, \quad \forall v \in H^1(\widehat{\Omega}_h), \quad \forall q \in H^{-1/2}(\Gamma_{\text{int}} \cup \partial\Omega). \end{aligned} \quad (2.9)$$

We call this form the general *hybrid formulation* for the embedded boundary problem.

The main difference between the two weak formulation (2.6) and (2.9) is, that in case of the general *Lagrange formulation*, the Lagrange multiplier  $\bar{p}$  for the embedded boundary is computed at the boundary  $\partial\Omega$  and vanishes for the solution  $u$  of the BVP (2.2), while in case of the general *hybrid formulation*,  $p$  is computed on  $\partial\widehat{\Omega}$  and  $p = \nabla u$ , for  $u$  satisfying the boundary value problem (2.2).

### 2.3 The stability of the Lagrange multiplier forms

For an initial consistency and stability study of the Lagrange-multiplier and the hybrid formulation for the embedded boundary condition, (2.6) and (2.9) respectively, we consider the following simple one-dimensional problem.

On a single cell, the unit interval  $\widehat{\Omega}_h = \widehat{\Omega} = (0, 1)$ , we consider the Poisson equation with homogeneous boundary conditions:

$$-\frac{d^2u}{dx^2} = f, \quad \text{on } \widehat{\Omega}, \quad \text{with } u(d) = 0, \quad u(1) = 0, \quad (2.10)$$

where  $d \in (0, 1)$  and  $\Omega = (d, 1)$ . To discretize (2.10), we take for test and trial spaces the  $(p + 1)$ -dimensional subspace  $S_h(\widehat{\Omega}) = P^p(\widehat{\Omega}) \subset H^1(\widehat{\Omega})$ , the polynomials of degree  $\leq p$ . So, we seek for the approximation

$$u_h = \sum_{0 \leq i \leq p} c_i \phi_i(x), \quad \phi_i(x) \in S_h(\widehat{\Omega}).$$

Because of the 1-D structure of this problem, boundary values on both  $\partial\Omega$  and  $\partial\widehat{\Omega}$  are parameterized by only two values. Therefore we provide the boundary spaces  $Q_h(\partial\widehat{\Omega}) \subset H^{-1/2}(\partial\widehat{\Omega})$  and  $Q_h(\partial\Omega) \subset H^{-1/2}(\partial\Omega)$  with the traces of two linear polynomials, viz.,  $Q_h(\partial\widehat{\Omega}) = \{\psi_0(x) = (1-x)|_{x=(0,1)}, \psi_1(x) = x|_{x=(0,1)}\}$  and  $Q_h(\partial\Omega) = \{\bar{\psi}_0(x) = \frac{x-1}{d-1}|_{x=(d,1)}, \bar{\psi}_1(x) = \frac{x-d}{1-d}|_{x=(d,1)}\}$ . Then the approximation of the two Lagrange multipliers is given by

$$p_h = \sum_{0 \leq i \leq 1} a_i \psi_i(x)|_{x=0,1} \quad \text{and} \quad \bar{p}_h = \sum_{0 \leq i \leq 1} a_i \bar{\psi}_i(x)|_{x=d,1}.$$

Having provided the approximation spaces, the two weak formulations (2.6) and (2.9), reduce to the following discrete weak forms:

(i) in case of the *Lagrange multiplier formulation*: find  $u_h \in S_h(\widehat{\Omega})$ ,  $\bar{p}_h \in Q_h(\partial\Omega)$  such that

$$\begin{aligned} \int_0^1 u'_h v'_h dx - [u'_h(1)v_h(1) - u'_h(0)v_h(0)] + [\bar{p}_h(1)v_h(1) - \bar{p}_h(d)v_h(d)] \\ + [q_h(1)u_h(1) - q_h(d)u_h(d)] = \int_0^1 v_h f dx, \quad \forall v_h \in S_h(\widehat{\Omega}), \quad q_h \in Q_h(\partial\Omega). \end{aligned} \quad (2.11)$$

(ii) in case of the *hybrid form*: find  $u_h \in S_h(\widehat{\Omega})$ ,  $p_h \in Q_h(\partial\widehat{\Omega})$  such that

$$\begin{aligned} \int_0^1 u'_h v'_h dx - [p_h(1)v_h(1) - p_h(0)v_h(0)] - [q_h(1)u_h(1) - q_h(d)u_h(d)] \\ = \int_0^1 v_h f dx, \quad \forall v_h \in S_h(\widehat{\Omega}), \quad q_h \in Q_h(\partial\Omega). \end{aligned} \quad (2.12)$$

First we study the consistency of the two discrete weak forms (2.11) and (2.12). So we check if we can solve for exact solutions in the polynomial space  $S_h(\widehat{\Omega})$ . The solution for  $f(x) = x^2$  in (2.10),  $d = 1/2$  and  $S_h(\widehat{\Omega}) = P^4(\widehat{\Omega})$  is shown in Figure 2. We see that the two formulations solve for the exact solution. The computed Lagrange multipliers are shown in Table 1. Here we see the main difference between the two methods: In case of the Lagrange

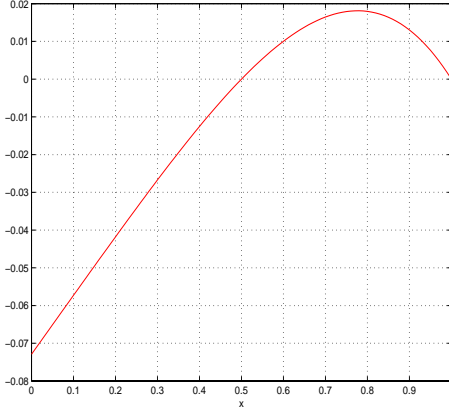


Figure 2: The solution  $u(x) = -\frac{1}{12}x^4 + \frac{5}{32}x - \frac{7}{96}$  computed with the hybrid- and Lagrange-method.

Lagrange method	(2.11)	$\bar{p}_h(d) = 0$	$\bar{p}_h(1) = 0$
hybrid method	(2.12)	$p_h(0) = 5/32$	$p_h(1) = -17/96$

Table 1: The values of the Lagrange multipliers of hybrid- and Lagrange- method for the solution as in Figure 2.

multiplier method, the Lagrange multipliers vanish at the boundary  $\partial\Omega$ , while in case of the hybrid method, the Lagrange multipliers correspond to the fluxes at the boundary of  $\partial\widehat{\Omega}$ , i.e.,  $p_h(x) = \frac{du_p}{dx}(x)$  for  $x = 0, 1$ .

Next we consider the stability of the two discrete weak formulations (2.11) and (2.12). So we check, if we can solve the BVP (2.10), for arbitrary locations of the embedded boundary condition  $d \in (0, 1)$  and arbitrary degree  $p$  of the polynomial space  $P^p(\widehat{\Omega})$ . Hence, for the two discrete weak formulations, we have to solve a  $(p+3) \times (p+3)$  linear system  $L_d u_h = f_h$ , where the matrix depends on the interior boundary location  $d$ . The results are shown in Table 2. We see that the Lagrange multiplier method has locations of the interior Dirichlet

The Lagrange method			
$p = 2$	$1/3$	—	—
$p = 3$	$2/5 - 1/10\sqrt{6}$	$2/5 + 1/10\sqrt{6}$	—
$p = 4$	0.08858795951	0.4094668644	0.7876594618

Table 2: Values for  $d$  for which the discrete system becomes singular. The discretisations are made for  $S_h(\widehat{\Omega}) = P^p(0, 1)$ ,  $p = 2, 3, 4$ .

boundary condition, for which the method becomes singular. The number of points where a singularity appears grows with increasing polynomial degree  $p$ . However, the hybrid method shows no singular points.

To study the singular behavior of the discrete Lagrange multiplier method more precisely,

we return to the equivalent discrete weak formulation of (2.11) with strongly imposed boundary conditions. Therefore, we consider the following function space of one-dimensional polynomials defined on  $\widehat{\Omega}_h = \widehat{\Omega} = (0, 1)$  such that

$$S_0(\Omega) = \left\{ u_h \in P^p(\widehat{\Omega}) \mid u_h(d) = u_h(1) = 0 \right\}. \quad (2.13)$$

Then the weak formulation, equivalent to (2.11), reads: find  $u_h \in S_0(\Omega)$  such that

$$\int_0^1 u'_h v'_h dx - [u'_h(1)v_h(1) - u'_h(0)v_h(0)] = \int_0^1 v_h f dx, \quad \forall v_h \in S_0(\Omega). \quad (2.14)$$

Consider now the discretisation of (2.14) with a quadratic polynomial basis. So we have  $S_0(\Omega) = \text{Span}\{\phi_0(x)\}$ , where  $\phi_0(x) = (x - d)(x - 1)$  and the approximation is given by  $u_h(x) = c_0\phi_0(x)$ . The form (2.14) reduces to a scalar equation  $L_h u_h = f_h$ , where the discrete operator  $L_h$  is given by  $L_h = \frac{1}{3} - d$ . We see immediately that a singularity appears if the interior Dirichlet boundary condition is located at  $d = 1/3$ . This singular point corresponds to the same location as shown in Table 2 for a third order discretisation of the Lagrange multiplier formulation.

For constant right-hand side  $f$  in the BVP (2.10), the solution of (2.14) reads

$$u_h = \frac{1}{2}f(x - d)(1 - x), \quad d \neq \frac{1}{3}, 1,$$

from which we conclude that this discretisation is third order consistent provided that  $d \in (0, 1) \neq \frac{1}{3}$ . The number of points where a singularity appears increases with the polynomial degree and the locations correspond with those of the Lagrange multiplier formulation as shown in Table 2.

From the formulation (2.14), we see that there exist locations  $d$  both for (2.11) and (2.14), for which the spurious mode in the solution satisfies the condition

$$\exists d \in (0, 1), \exists u_h \neq 0 \in S_0(\Omega) \mid \int_0^1 |u'_h|^2 dx = -u'_h(0)u_h(0), \quad (2.15)$$

with  $u'_h(0)u_h(0) \neq 0$ .

On the other hand, we can adapt formulation (2.14) such that the spurious modes, for arbitrary locations of the interior Dirichlet boundary condition  $d \in (0, 1)$ , are removed. Therefore, we introduce another space of one-dimensional polynomials defined on  $\widehat{\Omega}_h = \widehat{\Omega} = (0, 1)$ , such that

$$V_0(\widehat{\Omega}) = \left\{ v_h \in P^p(\widehat{\Omega}) \mid v_h(0) = v_h(1) = 0 \right\}, \quad (2.16)$$

and, we consider the following weak formulation: find  $u_h \in S_0(\Omega)$  such that

$$\int_0^1 u'_h v'_h dx = \int_0^1 v_h f dx, \quad \forall v_h \in V_0(\widehat{\Omega}), \quad (2.17)$$

where the polynomial space  $S_0(\Omega)$  is defined by (2.13). This formulation is also  $p + 1$  order consistent, and we see immediately, that for arbitrary  $d \in (0, 1)$  that, if

$$\exists d \in (0, 1), \exists u_h \neq 0 \in S_0(\Omega) \mid \int_0^1 u'_h, v'_h dx = 0, \quad \forall v_h \in V_0(\widehat{\Omega}),$$

$u_h$  must be a linear polynomial in  $S_0(\Omega)$ , i.e.,  $u_h \equiv 0$ . Hence, formulation (2.17) is stable for arbitrary locations of the interior Dirichlet boundary condition.

Summarizing, the Lagrange multiplier formulation for the embedded boundary condition (2.11) and hence (2.14), the equivalent formulation with strongly imposed interior Dirichlet boundary condition are unstable. The spurious modes in the solution of either (2.11) or (2.14) satisfy the condition (2.15). This instability is directly linked with the choice of test and trial space in formulation (2.14). If we take the trial space  $V_0(\widehat{\Omega})$ , as in (2.16), we arrive at a stable weak formulation with a strongly imposed interior Dirichlet boundary condition (2.17).

### 3. THE DISCONTINUOUS GALERKIN FORMS

#### 3.1 The Discontinuous Galerkin formulation for the embedded boundary condition

In the previous section we have seen that the discrete *hybrid formulation* for the one-dimensional Poisson equation on a single cell is stable. In [9], we also have shown, that third- and fourth order hybrid discretisations, for the two-dimensional Poisson equation on the unit cell with a curved embedded Dirichlet boundary condition, do not show locations of the embedded boundary condition for which the resulting linear system becomes unstable. So it appears to be appropriate to discretize a BVP with the hybrid method.

However, it appears that such a hybrid discretisation of the embedded BVP, on a multi-cell partitioning  $\widehat{\Omega}_h$ , as in (2.3), is rather complicated (besides the fact that such an discretisation is expensive, in view of the degrees of freedom for the Lagrange multiplier  $p$ ).<sup>2</sup>

To overcome this difficulty, we eliminate from (2.9) the Lagrange multiplier  $p \in H^{-1/2}(\widehat{\Gamma}_{\text{int}} \cup \partial\widehat{\Omega})$  and the extra test functions  $q \in H^{-1/2}(\Gamma_{\text{int}} \cup \partial\Omega)$ . Similar to the classical DG-technique [4, 5, 1, 18], where it is assumed that the Lagrange multiplier  $p$  on the common interface  $\widehat{\Gamma}_{\text{int}}$  corresponds with the average normal flux  $\langle \nabla u \rangle$  on that interface. Notice that in our case we have to distinguish between

$$\begin{aligned}\widehat{\Gamma}_{\text{int}} : \quad & \langle \tau(x) \rangle = \frac{1}{2} (\tau(x)|_{\partial\widehat{\Omega}_i} + \tau(x)|_{\partial\widehat{\Omega}_j}) \quad \text{and} \\ \Gamma_{\text{int}} : \quad & \langle \tau(x) \rangle = \frac{1}{2} (\tau(x)|_{\partial\Omega_i} + \tau(x)|_{\partial\Omega_j}).\end{aligned}\tag{3.1}$$

Recognizing that, for  $u$  satisfying (2.2), the Lagrange multiplier  $p$  in (2.9) equals  $\nabla u$  on the boundary  $\partial\widehat{\Omega}$ , and choosing  $q(\Gamma_{\text{int}}) = -\sigma \langle \nabla v \rangle - \mu[v]$  and  $q(\partial\Omega) = -\sigma \nabla v - \mu[v]$ , with jump operators<sup>3</sup> as in (2.5), we arrive at the *DG-formulation for the embedded boundary condition*:

---

<sup>2</sup>If, e.g., we want to have a fourth order discretisation of the (two-dimensional) hybrid formulation for the embedded boundary condition (2.9), we take for test and trial space  $S_h(\widehat{\Omega}_h) \subset H^1(\widehat{\Omega}_h)$  the usual space of piecewise cubic polynomials in each coordinate direction on the partitioning  $\widehat{\Omega}_h$ . However, we also have to define in (2.9) the finite dimensional subspaces  $Q_h(\widehat{\Gamma}_{\text{int}} \cup \partial\widehat{\Omega}) \subset H^{-1/2}(\widehat{\Gamma}_{\text{int}} \cup \partial\widehat{\Omega})$  and  $Q_h(\Gamma_{\text{int}} \cup \partial\Omega) \subset H^{-1/2}(\Gamma_{\text{int}} \cup \partial\Omega)$ . Since, as explained in [9], these subspaces are obtained from traces of cubic polynomials in  $Q_h(\widehat{\Omega}_h) \subset H^1(\widehat{\Omega}_h) \cap C^1(\widehat{\Omega}_h)$ , it is not trivial to find such a cubic polynomial space  $Q_h(\widehat{\Omega}_h)$  on the partitioning  $\widehat{\Omega}_h$ .

<sup>3</sup>At the boundaries  $\partial\widehat{\Omega}$  and  $\partial\Omega$  the interface with a virtual (flat, exterior) adjacent cell is used.

find  $u \in H^1(\widehat{\Omega}_h)$ , such that

$$\begin{aligned} & \sum_{\widehat{\Omega}_e \in \widehat{\Omega}_h} (\nabla u, \nabla v)_{\widehat{\Omega}_e} - \langle \nabla u, [v] \rangle_{\partial \widehat{\Omega}} + \sigma \langle \nabla v, [u] \rangle_{\partial \Omega} - \langle \langle \nabla u \rangle, [v] \rangle_{\widehat{\Gamma}_{\text{int}}} \\ & + \sigma \langle \langle \nabla v \rangle, [u] \rangle_{\widehat{\Gamma}_{\text{int}}} + \mu \langle [v], [u] \rangle_{\widehat{\Gamma}_{\text{int}} \cup \partial \Omega} = \sum_{\widehat{\Omega}_e \in \widehat{\Omega}_h} (f, v)_{\widehat{\Omega}_e} + \sigma \langle \nabla v, [u_0] \rangle_{\partial \Omega} \\ & + \mu \langle [v], [u_0] \rangle_{\partial \Omega}, \quad \forall v \in H^1(\widehat{\Omega}_h). \end{aligned} \quad (3.2)$$

Notice that (3.2) can also be obtained from (2.6). If we substitute in (2.6)  $\bar{p}(\partial \Omega) \equiv 0$ ,  $p(\widehat{\Gamma}_{\text{int}}) = \langle \nabla u \rangle$ ,  $q(\Gamma_{\text{int}}) = -\sigma \langle \nabla v \rangle - \mu[v]$  and  $q(\partial \Omega) = -\sigma \nabla v - \mu[v]$ , we also arrive at (3.2).

In the following section we study the stability of (3.2).

### 3.2 The instability of the Discontinuous Galerkin formulation

For an initial stability study of (3.2) we return again to the one-dimensional equation on a single cell with an interior Dirichlet boundary condition. So, considering (2.10), the general DG-formulation for the embedded boundary condition reduces to: find  $u_h \in S_h(\widehat{\Omega})$  such that

$$\begin{aligned} & \int_0^1 u'_h v'_h dx - [u'_h(1)v_h(1) - u'_h(0)v_h(0)] + \sigma [u_h(1)v'_h(1) - u_h(d)v'_h(d)] \\ & + \mu [u_h(1)v_h(1) + u_h(d)v_h(d)] = \int_0^1 v_h f dx, \quad \forall v_h \in S_h(\widehat{\Omega}_h), \end{aligned} \quad (3.3)$$

where the  $S_h(\widehat{\Omega}) = P^p(\widehat{\Omega}) \subset H^1(\widehat{\Omega})$  is the  $(p+1)$ -dimensional space of polynomials of degree  $\leq p$  and the approximation is given by

$$u_h = \sum_{0 \leq i \leq p} c_i \phi_i(x), \quad \phi_i(x) \in S_h(\widehat{\Omega}).$$

It is obvious that (3.3) is  $(p+1)$ -order consistent.

However, similar as for (2.11), stability of (3.3) is not guaranteed for arbitrary locations  $d \in (0, 1)$ . For given a given polynomial basis in  $S_h(\widehat{\Omega})$  we have to solve a  $(p+1) \times (p+1)$  linear system  $L_{\sigma, \mu, d} u_h = f_h$ , in which the matrix depends on the method parameter  $\sigma = \pm 1$ , the penalty parameter  $\mu \geq 0$  and the location of the interior Dirichlet boundary condition  $d$ . The locations  $d$ , for which the resulting linear system of the Baumann-Oden-DG ( $\sigma = 1, \mu = 0$ ), the symmetric-DG ( $\sigma = -1, \mu = 0$ ) and the non-symmetric interior penalty-method (NIPG) ( $\sigma = 1, \mu > 0$ ), are singular, are shown in Table 3. Also in these cases, we see that the number of locations of the interior Dirichlet boundary condition for which the discrete system becomes singular, increases with the polynomial degree  $p$ . The use of the penalty parameter  $\mu > 0$  does not stabilize the method. We discuss this below.

Consider the NIPG formulation in (3.3) with  $\sigma = 1$  and  $\mu \gg 1$ . Apparently, there are values of  $d$ , such that a spurious mode in (3.3) exists:

$$0 \neq u_h \in S_h(\widehat{\Omega}_h) \mid \int_0^1 |u'_h|^2 dx + u'_h(0)u_h(0) - u_h(d)u'_h(d) + \mu[u_h^2(1) + u_h^2(d)] = 0. \quad (3.4)$$

For  $\mu \gg 1$ , we may simplify formulation (3.4) into

$$0 \neq u_h \in S_h(\widehat{\Omega}_h) \mid \int_0^1 |u'_h|^2 dx + u'_h(0)u_h(0) + \mu[u_h^2(1) + u_h^2(d)] = 0, \quad (3.5)$$

The symmetric- / Baumann-method ( $\sigma = \pm 1, \mu = 0$ )			
$p = 2$	—	—	—
$p = 3$	$2/5$	—	—
$p = 4$	$3/7 - 1/7\sqrt{2}$	$3/7 + 1/7\sqrt{2}$	—

NIPG ( $\sigma = 1, \mu = 5$ )			
$p = 2$	$11/21$	—	—
$p = 3$	0.2820018914	0.8313042416	—
$p = 4$	0.1786866021	0.5490461868	0.934889434

Table 3: Values for  $d$  for which the discrete system becomes singular. The discretisations are made for  $S_h(\widehat{\Omega}) = P^p(0, 1)$ ,  $p = 2, 3, 4$ .

and, we see that in the limit for  $\mu \rightarrow \infty$  a spurious mode for (3.3) exists:

$$\exists u_h \neq 0 \in S_h(\widehat{\Omega}_h), u_h(d) = u_h(1) = 0 \mid \int_0^1 |u'_h|^2 dx = -u'_h(0)u_h(0), \quad (3.6)$$

with  $u'_h(0)u_h(0) \neq 0$ . Hence, the NIPG method in (3.3) with large penalty parameter  $\mu$  is unstable for a  $d$  satisfying (3.6). Notice that (3.6) is equivalent to condition (2.15), for which the discrete Lagrange multiplier formulation (2.11) is unstable.

Figure 3 shows the two spurious modes of a fourth order NIPG discretisation according to (3.3), with  $\sigma = 1$  and  $\mu \gg 1$ . We see that the functions satisfy the conditions  $u_h(d) = u_h(1) = 0$  and that the locations  $d \in (0, 1)$ , coincide with the two locations, as shown in Table 2, for which the fourth order discrete Lagrange multiplier formulation (2.11) is unstable.

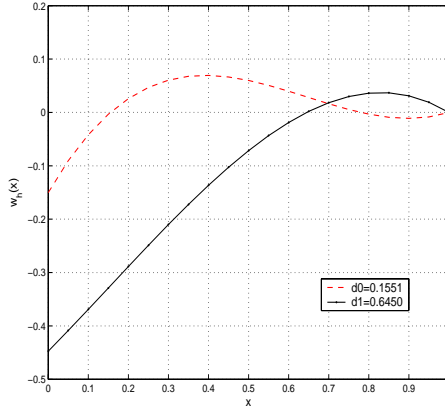


Figure 3: The two spurious modes of a fourth order NIPG discretisation, according to (3.3) with  $\sigma = 1$  and  $\mu \gg 1$ . The functions satisfy the homogeneous Dirichlet boundary conditions  $u_h(d) = u_h(1) = 0$ , where the locations  $d \approx 2/5 \pm 1/10\sqrt{6}$  correspond to the values of  $d$  for which also the fourth order Lagrange multiplier discretisation is unstable, as shown in Table 2.

### 3.3 A stability fix of the Baumann-Oden variant

Now we introduce a *modified DG formulation* for the one-dimensional problem defined in (2.10).

For this purpose, we split the space  $V(\widehat{\Omega}) = H^1(\widehat{\Omega})$  as

$$V(\widehat{\Omega}) = P^1(\widehat{\Omega}) \oplus H_0^1(\widehat{\Omega}), \quad (3.7)$$

where  $P^1(\widehat{\Omega}) = \text{Span}\{1 - x, x\}$ . And we introduce the following trace operator on the embedded boundary at  $x = d$ :

$$\tilde{\gamma}_d : V(\widehat{\Omega}) \rightarrow P^1(d) \subset H^{-1/2}(d) : \tilde{\gamma}_d(v) = \tilde{\gamma}_d(v_0 + v_1) = v_0(d), \quad (3.8)$$

with  $v_0 \in P^1(\widehat{\Omega})$  and  $v_1 \in H_0^1(\widehat{\Omega})$ . Next, we introduce the weak formulation: find  $u \in V(\widehat{\Omega})$  such that

$$\begin{aligned} B(u, v) &\equiv \int_0^1 u'v' dx + u'(0)v(0) - u'(1)v(1) + v'(1)u(1) \\ &\quad + \tilde{\gamma}_d(v)u(d) = \int_0^1 fv dx, \quad \forall v \in V(\widehat{\Omega}). \end{aligned} \quad (3.9)$$

It is obvious that, if for arbitrary  $d \in (0, 1)$  a solution  $u \in V$  satisfying (2.10), the solution also satisfies (3.9). Next we show that the solution  $u \in V(\widehat{\Omega})$  of (3.9) is unique and hence satisfies (2.10).

**Theorem 1.** Consider the bilinear form  $B(u, v)$  given in (3.9) on the functions space  $V(\widehat{\Omega})$  as in (3.7). The form  $B(u, v)$  is stable, in the sense that, for arbitrary  $d \in (0, 1)$ , from  $B(u, v) = 0, \forall v \in V(\widehat{\Omega})$  it follows that  $u \equiv 0$ .

*Proof.* Let  $0 \neq u \in V(\widehat{\Omega})$  be arbitrary and select first  $v_1 \in D(\widehat{\Omega}) = \{v \in H_0^1(\widehat{\Omega}), v'(1) = 0\}$ . From

$$\int_0^1 u'v'_1 dx = 0, \quad \forall v_1 \in D(\widehat{\Omega}) \subset H_0^1(\widehat{\Omega}), \quad (3.10)$$

we conclude that  $u$  is a linear polynomial on  $\widehat{\Omega}$ . Next, for arbitrary  $v_1 \in H_0^1(\widehat{\Omega})$ ,

$$\int_0^1 u'v'_1 dx + u(1)v'_1(1) = 0, \quad (3.11)$$

so that  $u = a_0(1 - x) \in P^1(\widehat{\Omega}) \subset V(\widehat{\Omega})$ ,  $a_0 \in \mathbb{R}$ , satisfying the homogeneous Dirichlet boundary condition  $u(1) = 0$ . Now, we consider the last condition in the sense that for  $u = a_0(1 - x)$ , we still have to satisfy

$$\int_0^1 u'v'_0 dx + u'(0)v_0(0) - u'(1)v_0(1) + v_0(d)u(d) = 0, \quad \forall v_0 \in P^1(\widehat{\Omega}). \quad (3.12)$$

Notice that for  $u = a_0(1 - x)$  and  $v_0 = 1 - x$  or  $v_0 = x$ , the first three terms in (3.12) vanish. Hence we are left over with the condition that  $u(d)v_0(d) = 0$ ,  $\forall v_0 \in P^1(\widehat{\Omega})$ , and hence  $u \equiv 0$ . Or  $B(u, v) = 0, \forall v \in V(\widehat{\Omega})$  implies that  $u \equiv 0$ .  $\square$

The bilinear form (3.9) also has two coercivity properties, which are listed below.

- i) If  $u \in H_0^1(\widehat{\Omega})$ , we have immediately that  $\forall u \in H_0^1(\widehat{\Omega}), B(u, u) \geq \gamma \|u'\|_{L_2(\widehat{\Omega})}$ ,  $\gamma > 0$ .
- ii) For  $u, v_0 \in P^1(\widehat{\Omega})$  in (3.7), we associate the bilinear form (3.9) with a  $2 \times 2$  linear system from which we derive the eigenvalues:

$$\lambda_{1,2} = 1 - d + d^2 \pm \sqrt{d^4 - 2d^3 + 3d^2 - d}.$$

We see that for  $d \in (0, 1)$ , the real part of both eigenvalues is positive. In view of the properties (i) and (ii), we assume that the operator  $B(u, v)$  of (3.9) is positive definite.

To study the discretisation of (3.9) in practice, we take for test and trial space  $S(\widehat{\Omega}) = \text{Span}\{\phi_i(x)\} \subset V(\widehat{\Omega})$ ,  $i = \{0, 1, \dots, 2p - 1\}$  the polynomials of degree less than  $2p$ , where on the unit interval we consider the following polynomials

$$\begin{aligned} \phi_0(t) &= 1 - t, \quad \phi_1(x) = t, \\ \phi_{2n+k} &= -t^{n+k}(1-t)^{n+1-k}, \quad n = 1, \dots, p-1, \quad k = 0, 1. \end{aligned} \tag{3.13}$$

Then with the approximation  $u_h = \sum_{0 \leq i \leq 2p-1} c_i \phi_i(x)$ , the discretisation of (3.9) reduces to a  $2p \times 2p$  linear system  $L_h u_h = f_h$ . Figure 4 shows the spectrum in the complex domain as function of  $d \in (0, 1)$  for the fourth order discretisation of (3.9) with polynomial basis (3.13) and  $p = 2$ . We see that for arbitrary  $d \in (0, 1)$  the real part of the eigenvalues is positive. The discrete operator is well conditioned for values of  $d$  up to 0.75. For  $d$  close to one, the matrix becomes singular, which is directly a consequence of the vanishing domain of interest  $\Omega$  [9]. Also higher order discretisations of (3.9) with polynomial basis (3.13) show positive definite spectra for arbitrary  $d \in (0, 1)$ . Numerical experiments of

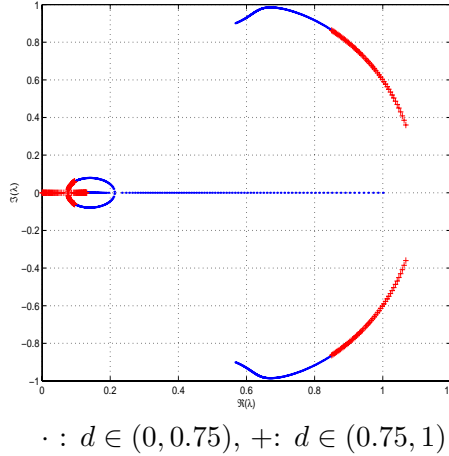


Figure 4: The spectrum  $\lambda_i$ ,  $i = (0, 1, \dots, 3)$  in the complex domain as function of the embedded boundary location  $d \in (0, 1)$  of the fourth-order discretisation of (3.9) with polynomial basis (3.13).

the one-dimensional Poisson equation on more cells, where 'normal' cells, which have no embedded boundary, are discretized with the Baumann-Oden DG-method and cells with the embedded Dirichlet boundary condition with the modified DG-method (3.9), also show that the resulting linear system is positive definite. This motivates us to continue with two-dimensional experiments.

#### 4. THE TWO-DIMENSIONAL CASE

##### 4.1 The stability of a two-dimensional DG-discretisation for the Poisson equation on a cell

Having studied the stability and consistency of DG-discretisations for the one-dimensional Poisson equation with an interior Dirichlet boundary condition, we now study fourth-order DG-discretisations for the two-dimensional Poisson equation with a similar embedded boundary condition.

Starting from (3.2), the Baumann-Oden formulation for the Poisson equation with embedded boundary condition ( $\sigma = 1$ ,  $\mu = 0$ ), the idea is to stabilize cells having an interior boundary segment by means of an extra weight in order to arrive at a linear system in which the discrete operator is positive definite.

Consider for this purpose the following BVP. On a single unit square  $\widehat{\Omega}$ , we define the Poisson equation with Dirichlet boundary condition on  $\Gamma_D$  and interior boundary part  $\gamma$

$$-\Delta u = f \quad \text{on } \widehat{\Omega}, \quad \text{and} \quad u = u_0 \quad \text{on } \partial\Omega = \Gamma_D \cup \gamma, \quad (4.1)$$

where the Dirichlet boundary conditions are defined on

$$\begin{aligned} \Gamma_D &= \{(x, y) \mid 0 < x < d, y = 0, 1; x = 0, 0 < y < 1\}, \\ \gamma &= \{(x, y) \mid x = d, 0 < y < 1\}. \end{aligned}$$

To discretize (4.1), we take for the finite dimensional test and trial space  $S_h(\widehat{\Omega}) \subset H^1(\widehat{\Omega})$  the space of cubic tensor-product polynomials in each of the two coordinate directions, based on (3.13). Hence, with

$$S_h(\widehat{\Omega}_h) = \left\{ \phi_{j,e}(y)\phi_{i,e}(x) \in P^{3 \times 3}(\widehat{\Omega}) \right\}, \quad (4.2)$$

and the approximation

$$u_h(x, y) = \sum_{0 \leq i,j \leq 4} c_{i,j} \phi_i(x) \phi_j(y), \quad (4.3)$$

we consider, according to (3.2), the following discrete weak formulation for the BVP (4.1): find  $u_h \in S_h(\widehat{\Omega})$  such that

$$\begin{aligned} (\nabla u_h, \nabla v_h)_{\widehat{\Omega}} - \langle \mathbf{n} \cdot \nabla u_h, v_h \rangle_{\partial\widehat{\Omega}} + \langle \mathbf{n} \cdot \nabla v_h, u_h \rangle_{\partial\Omega} + \text{PE}_\gamma(u_h, v_h) \\ = (f, v_h)_{\widehat{\Omega}} + \langle \mathbf{n} \cdot \nabla v_h, u_0 \rangle_{\partial\Omega} + \text{PE}_\gamma(u_0, v_h), \quad \forall v_h \in S_h(\widehat{\Omega}), \end{aligned} \quad (4.4)$$

where  $\text{PE}_\gamma(\cdot, \cdot)$  is respectively a penalty and weighting term on the interior boundary  $\gamma$ , which we specify below. For this initial stability study we consider either

$$\text{PE}_\gamma(u_h, v_h) = \mu \langle u_h, v_h \rangle_\gamma, \quad \text{or} \quad (4.5)$$

$$\text{PE}_\gamma(u_h, v_h) = \mu \langle u_h, \tilde{\gamma}_D(v_h) \rangle_\gamma, \quad (4.6)$$

where  $\mu = \nu/|\gamma|$ ,  $|\gamma|$  the interior boundary length and  $\tilde{\gamma}_D(v_h)$  is a trace operator similar to (3.8) and here defined by

$$\tilde{\gamma}_D : S_h(\widehat{\Omega}) \subset H^1(\widehat{\Omega}) \rightarrow P^{1 \times 1}(\gamma) \subset H^{-1/2}(\gamma) : \tilde{\gamma}_D(v_h) = v_{0,h}(\gamma) \in P^{1 \times 1}(\gamma), \quad (4.7)$$

and  $P^{1 \times 1}(\gamma) = \{v_h \mid v_h = v_h|_\gamma, v_h \in P^{1 \times 1}\}$  i.e.,  $P^{1 \times 1}(\gamma)$  contains functions that are restrictions of a bilinear function on  $\widehat{\Omega}$  to the embedded boundary  $\gamma$ . In this way, applying the extra weight (4.6) in the weak formulation (4.4) means that the interior boundary  $\gamma$  is weighted with the traces of only the linear polynomials in  $S_h(\widehat{\Omega})$ , whereas using the penalty term (4.5) means that, the interior boundary is penalized with traces of *all* polynomials in  $S_h(\widehat{\Omega})$ .

With the finite dimensional function space (4.2) and the approximation (4.3), the bilinear form (4.4) reduces to a  $16 \times 16$  linear system  $L_h u_h = f_h$ , in which the discrete operator  $L_h$  is still a function of  $d$ , the location of the interior Dirichlet boundary condition. For the penalty term (4.5) and weight (4.6), with  $\mu = 0, 5$  and  $10$ , Figure 5 shows the spectral condition number  $\kappa$  as function of  $d$ . If we first consider in this figure form (4.4) with the extra weight

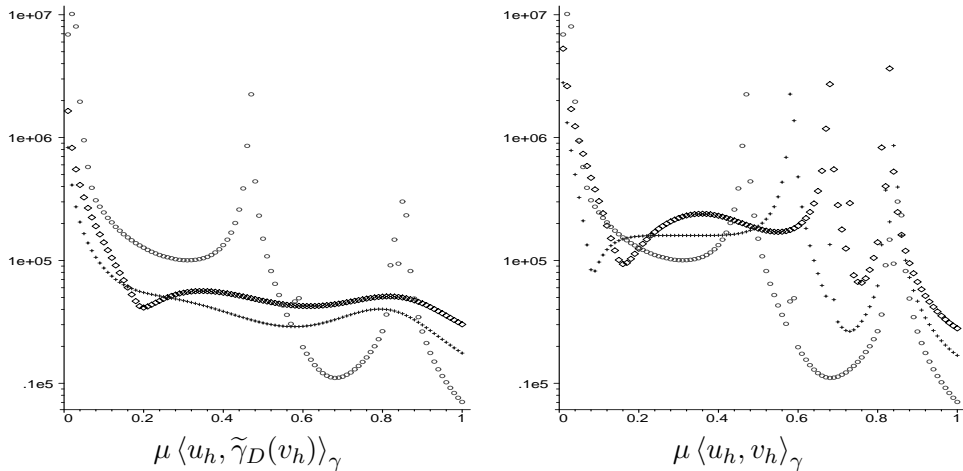


Figure 5: The condition number  $\kappa$  of the discrete operator as function of  $d$ , the location of the interior boundary condition. The  $16 \times 16$  linear system arises from the discrete formulation (4.4) with either penalty term (4.5) or weight (4.6) on the interior boundary  $\gamma$ .  $\circ$ :  $\mu = 0$ ,  $+$ :  $\mu = 5$  and  $\diamond$ :  $\mu = 10$ .

(4.6), we see that in case  $\mu = 0$  there are locations of the embedded boundary for which the discrete system  $L_h u_h = f_h$  is singular. However, these locations vanish for increasing values of the parameter  $\mu$ . The situation changes if the interior boundary is penalized by (4.5). Although in this case the singular locations appear to be a function of  $\mu$ , they do not vanish.

Figure 6 shows the smallest real part of the eigenvalues in the spectrum of  $L_h$  with weight (4.6) as function  $d$ . We see that the discrete operator  $L_h$  is positive definite for arbitrary location  $0 < d < 1$  of the interior boundary. The effect of the parameter  $\mu$  is small, although  $\min(\Re(\lambda_i))$  is somewhat larger in the range  $0.4 < d < 1$  for  $\mu = 10$ .

So, in view of this fourth-order discretisation of (4.4), the weight (4.6) stabilizes the discrete operator  $L_h$  in a similar way as in the one-dimensional case. However, for discretisations of (4.4) of order higher than four, a more sophisticated weighting term should be introduced, to remove spurious modes in the solution.

Nevertheless this result motivates us to continue studying this technique for more complex domains partitioned according to (2.3), where the cells with interior boundary segments are discretized by the fourth-order discrete form (4.4) with weight (4.6) and other cells are discretized by means of Baumann-Oden's DG form, expecting that the overall linear system

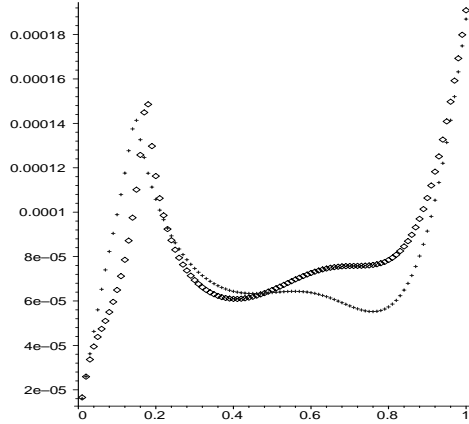


Figure 6: The smallest real part,  $\min_{i=0,1..,15}(\Re(\lambda_i))$ , of the eigenvalues in the spectrum of  $L_h$  corresponding with (4.4) and weight (4.6), as function of the interior boundary location  $d$ .  $+$ :  $\mu = 5$  and  $\diamond$ :  $\mu = 10$ .

$L_h u_h = f_h$  will be positive definite.

*4.2 Application to the Poisson equation on a rectangle domain with a halve circle excluded*  
In this section we study a fourth order discretisation of the Baumann-Oden DG formulation (3.2), with  $\sigma = 1$ ,  $\mu = 0$ , for the two-dimensional Poisson equation on a rectangular domain with a halve circle excluded, where we apply on the interior boundary the extra weight (4.6).

For this purpose, we consider the (initial) computational domain  $\widehat{\Omega}$  with vertices  $(x, y) = (0, 0), (2, 0), (2, 1)$  and  $(2, 2)$ . The circular embedded boundary is described by

$$\gamma = \{(x, y) \mid (x - 1)^2 + y^2 = R^2 < 1, x, y \geq 0\}. \quad (4.8)$$

So, the fictitious part of the domain  $\widehat{\Omega}$  is given by

$$\widetilde{\Omega} = \{(x, y) \mid x, y \geq 0, (x - 1)^2 + y^2 < R^2\}.$$

Next, according to (2.3), we partition the domain  $\widehat{\Omega}$  in a set of regular square dyadic grids  $\{g(i), i = 0, 1, 2, 3\}$ , with mesh size  $h = h_x = h_y = (\frac{1}{2})^i$ . An example of such partitionings is shown in Figure 7. In this figure, we see the coarse and finer partitionings, where the radius of the embedded boundary is  $R = \sqrt{0.13}$ . We take the radius in (4.8) such that the circular curve segments  $\gamma_e$  in cells  $\widehat{\Omega}_e$  intersect two edges, and such that the local domains of interest  $\Omega_e$  in cells  $\widehat{\Omega}_e$  do not vanish.

On partitionings as in Figure 7, we consider the discrete Baumann-Oden DG formulation for the embedded boundary (3.2) with weight (4.6): find  $u_h \in S_h(\widehat{\Omega}_h)$  such that

$$\begin{aligned} & \sum_{\widehat{\Omega}_e \in \widehat{\Omega}_h} (\nabla u_h, \nabla v_h)_{\widehat{\Omega}_e} - \langle \mathbf{n} \cdot \nabla u_h, v_h \rangle_{\partial \widehat{\Omega}} + \langle \mathbf{n} \cdot \nabla v_h, u_h \rangle_{\partial \Omega} - \langle \langle \nabla u_h \rangle, [v_h] \rangle_{\Gamma_{int}} \\ & + \langle \langle \nabla v_h \rangle, [u_h] \rangle_{\Gamma_{int}} + \mu \langle \tilde{\gamma}_D(v_h), u_h \rangle_{\gamma} = \sum_{\widehat{\Omega}_e \in \widehat{\Omega}_h} (f, v_h)_{\widehat{\Omega}_e} + \langle \mathbf{n} \cdot \nabla v_h, u_0 \rangle_{\partial \Omega} \\ & + \mu \langle \tilde{\gamma}_D(v_h), u_0 \rangle_{\gamma}, \quad \forall v_h \in S_h(\widehat{\Omega}_h), \end{aligned} \quad (4.9)$$

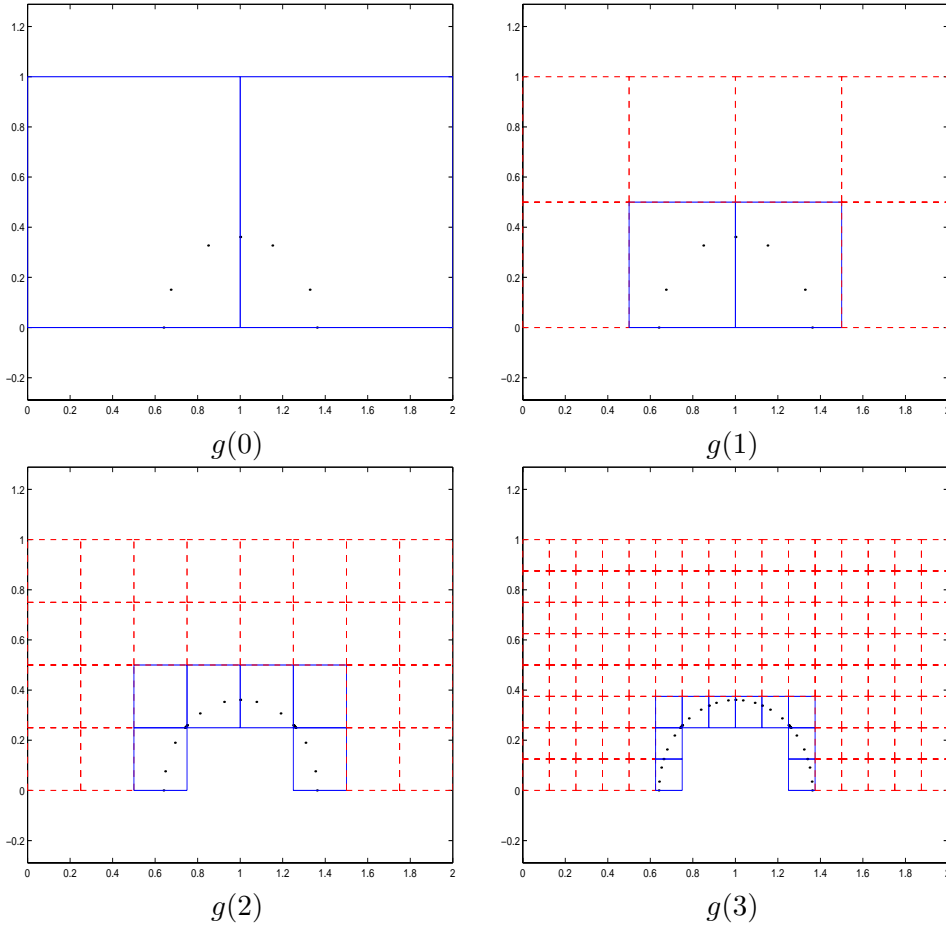


Figure 7: The domain  $\widehat{\Omega}$ , partitioned in  $\{g(i), i = 0, 1, 2, 3\}$ , with a halve circle excluded. The embedded boundary is described by  $\gamma = \{(x, y) \mid (x - 1)^2 + y^2 = R^2 < 1, x, y \geq 0\}$ . In this example, is the radius  $R = \sqrt{0.13}$ . Along each circle segment,  $\gamma_e$ , per cell  $\widehat{\Omega}_e$ , to compute the boundary integrals four-point Lobatto quadrature is used (black dots).

where  $\mu = \nu/|\gamma_e|$ ,  $\nu > 0$  and  $\gamma = \sum_e \gamma_e$  with  $\gamma_e$  the boundary segment in cell  $\widehat{\Omega}_e$ .

Next, we take for the finite dimensional test and trial space  $S_h(\widehat{\Omega}_h) \subset H^1(\widehat{\Omega}_h)$  the space of piecewise cubic tensor-product polynomials as in (4.2). On the master square  $[0, 1]^2 \subset \mathbb{R}^2$ , we use as a basis the tensor-product polynomials based on (3.13), which is partly hierarchical. A basis for  $P^{3 \times 3}(\widehat{\Omega}_e)$  is obtained by the usual affine mapping  $[0, 1]^2 \rightarrow \widehat{\Omega}_e$ . Hence on the regular grid in Figure 7 the approximate solution is:

$$\begin{aligned} u_h(x, y) &= \sum_{1 \leq e \leq N} \sum_{0 \leq i, j < 4} c_{e,i,j} \phi_i\left(\frac{x - x_e}{h_x}\right) \phi_j\left(\frac{y - y_e}{h_y}\right) \\ &\equiv \sum_{1 \leq e \leq N} \sum_{0 \leq i, j < 4} c_{e,i,j} \phi_{e,i}(\xi) \phi_{e,j}(\eta). \end{aligned} \quad (4.10)$$

The linear system  $L_h u_h = f_h$  arising from (4.9) is obtained in explicit form if we consider  $M$  'normal' cells and  $N - M$  cells with an interior boundary segment  $\gamma_e$ . Then, computing

the boundary terms in cells with an interior boundary segment with four-point Lobatto quadrature, we arrive at the discrete system

$$\begin{aligned}
& \sum_{1 \leq e \leq M} \sum_{0 \leq i, j < 4} c_{e,i,j} \left[ \left( \frac{1}{h_x} \int_0^1 \phi'_{e,i} \phi'_{e,\tilde{i}} d\xi - \frac{1}{h_x} \langle \nabla \phi_{e,i} \rangle \cdot [\phi_{e,\tilde{i}}] \right|_{\hat{\Gamma}_{int} \cup \partial \hat{\Omega}} + \right. \\
& \quad \left. \frac{1}{h_x} [\phi_{e,i}] \cdot \langle \nabla \phi_{e,\tilde{i}} \rangle \Big|_{\hat{\Gamma}_{int} \cup \partial \hat{\Omega}} \right) h_y \int_0^1 \phi_{e,j} \phi_{e,\tilde{j}} d\eta + \\
& \quad h_x \int_0^1 \phi_{e,i} \phi_{e,\tilde{i}} d\xi \left( \frac{1}{h_y} \int_0^1 \phi'_{e,j} \phi'_{e,\tilde{j}} d\eta - \frac{1}{h_y} \langle \nabla \phi_{e,j} \rangle \cdot [\phi_{e,\tilde{j}}] \right|_{\hat{\Gamma}_{int} \cup \partial \hat{\Omega}} + \\
& \quad \left. \frac{1}{h_y} [\phi_{e,j}] \cdot \langle \nabla \phi_{e,\tilde{j}} \rangle \Big|_{\hat{\Gamma}_{int} \cup \partial \hat{\Omega}} \right) \\
& \quad + \\
& \sum_{M < e \leq N} \sum_{0 \leq i, j < 4} c_{e,i,j} \left[ \left( \frac{1}{h_x} \int_0^1 \phi'_{e,i} \phi'_{e,\tilde{i}} d\xi - \frac{1}{h_x} \langle \nabla \phi_{e,i} \rangle \cdot [\phi_{e,\tilde{i}}] \right|_{\hat{\Gamma}_{int} \cup \partial \hat{\Omega}} \right) h_y \int_0^1 \phi_{e,j} \phi_{e,\tilde{j}} d\eta + \\
& \quad h_x \int_0^1 \phi_{e,i} \phi_{e,\tilde{i}} d\xi \left( \frac{1}{h_y} \int_0^1 \phi'_{e,j} \phi'_{e,\tilde{j}} d\eta - \frac{1}{h_y} \langle \nabla \phi_{e,j} \rangle \cdot [\phi_{e,\tilde{j}}] \right|_{\hat{\Gamma}_{int} \cup \partial \hat{\Omega}} + \\
& \quad \sum_{\Gamma_{\tilde{e}} \in \partial \Omega_e \cap \Gamma_{int}} \sum_{0 \leq k < 4} w_k |\Gamma_{\tilde{e}}| \left\langle \nabla \left( \phi_{e,\tilde{i}} \left( \frac{x(s_k) - x_e}{h_x} \right) \phi_{e,\tilde{j}} \left( \frac{y(s_k) - y_e}{h_y} \right) \right) \right\rangle \cdot \left[ \phi_{e,i} \left( \frac{x(s_k) - x_e}{h_x} \right) \phi_{e,j} \left( \frac{y[s_k] - y_e}{h_y} \right) \right] + \\
& \quad \sum_{\Gamma_{\tilde{e}} \in \partial \Omega_e \cap \partial \Omega \setminus \gamma} \sum_{0 \leq k < 4} w_k |\Gamma_{\tilde{e}}| \left( \mathbf{n}_k \cdot \nabla \left( \phi_{e,\tilde{i}} \left( \frac{x(s_k) - x_e}{h_x} \right) \phi_{e,\tilde{j}} \left( \frac{y(s_k) - y_e}{h_y} \right) \right) \right) \left( \phi_{e,i} \left( \frac{x(s_k) - x_e}{h_x} \right) \phi_{e,j} \left( \frac{y[s_k] - y_e}{h_y} \right) \right) + \\
& \quad \nu \sum_{0 \leq k < 4} w_k \tilde{\gamma}_D \left( \phi_{e,\tilde{i}} \left( \frac{x(s_k) - x_e}{h_x} \right) \phi_{e,\tilde{j}} \left( \frac{y(s_k) - y_e}{h_y} \right) \right) \left( \phi_{e,i} \left( \frac{x(s_k) - x_e}{h_x} \right) \phi_{e,j} \left( \frac{y[s_k] - y_e}{h_y} \right) \right) \\
= & \sum_{1 \leq e \leq N} \sum_{0 \leq i, j < 4} \left[ \int_{\hat{\Omega}_e} f(x, y) \phi_{\tilde{i}} \left( \frac{x - x_e}{h_x} \right) \phi_{\tilde{j}} \left( \frac{y - y_e}{h_y} \right) d\hat{\Omega}_e \right] + \\
& \quad \sum_{\Gamma_e \in \partial \Omega \setminus \gamma} \sum_{0 \leq k < 4} w_k |\Gamma_e| \mathbf{n}_k \cdot \nabla \left( \phi_{\tilde{i}} \left( \frac{x(s_k) - x_e}{h_x} \right) \phi_{\tilde{j}} \left( \frac{y(s_k) - y_e}{h_y} \right) \right) u_0 + \\
& \quad \nu \sum_{\gamma_e \in \gamma} \sum_{0 \leq k < 4} w_k \tilde{\gamma}_D \left( \phi_{e,\tilde{i}} \left( \frac{x(s_k) - x_e}{h_x} \right) \phi_{e,\tilde{j}} \left( \frac{y(s_k) - y_e}{h_y} \right) \right) u_0, \quad 0 \leq \tilde{i}, \tilde{j} < 4.
\end{aligned} \tag{4.11}$$

Here, for some constant  $\nu > 0$  on each interior boundary segment,  $\mu = \nu/|\gamma_e|$ . Notice that in cells  $\hat{\Omega}_e$  with an interior boundary segment, continuity of the approximation  $u_h$  is only required on the edges  $\Gamma_{\tilde{e}} \cap \partial \Omega_e$ . To compute the integrals over these (partial, rectangular) edges, four-point Lobatto quadrature is used. Also for computing the integrals over the interior boundary segments  $\gamma_e$  of the curved embedded boundary  $\gamma$ , we apply four-point Lobatto quadrature as shown in Figure 7. Here denote  $\mathbf{n}_k$  the unit outward normal evaluated at the quadrature point  $s_k$ . The other terms in (4.11), are direct extensions of one-dimensional mass and stiffness matrices discussed in [10] and can be straight-forwardly computed.

By construction (4.11) is fourth-order consistent, both in the interior of the domain  $\Omega$  and on the wall  $\partial \Omega$ , independently of the choice of the constant  $\nu$ . Figure 8 confirms this observation. Here we see the approximation computed by (4.11) for the BVP (2.2) with right-hand side and boundary conditions such that the solution is given by  $u = 4xy(x-2)(y-1)$ . We observe that indeed (4.11) can solve for the exact solution (except for rounding errors) on the domain of interest  $\Omega$ .

Next we test the convergence of the discrete system (4.11), where we distinguish two cases:  $\nu = 0$  and  $\nu = 10$ , in order to see the influence of the weight (4.6) on (4.11). For this purpose,

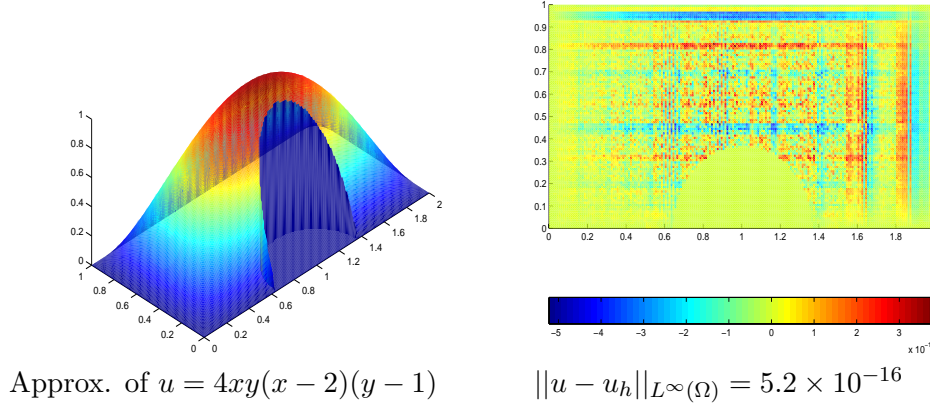


Figure 8: The solution and the error on the domain  $\Omega$  of the problem  $\Delta u = 8(y(y-1) + x(x-2))$  discretized by the fourth order DG-discretisation (4.11) for the embedded boundary condition with  $\nu = 0$ . The discretisation is made on grid  $g(1)$  as shown in Figure 7. The radius of the circular embedded boundary is  $R = \sqrt{0.13}$ .

we choose the right-hand side and the boundary conditions in (2.2) such that the solution is  $u = \sin(x)\cos(y)$ . On the four grids  $\{g(0), \dots, g(3)\}$  as in Figure 7, and for radii  $R = \sqrt{0.13}$  and  $R = \sqrt{0.50}$ , we compute the error  $\|u - u_h\|_{L^\infty(\Omega)}$  of the approximations, by evaluating the difference between the exact and computed solution on a  $50 \times 50$  equidistant grid per cell  $\hat{\Omega}_e$ . On the fictitious part of a cell  $\hat{\Omega}_e$  we define the error to be zero. Furthermore we compute the spectral condition number  $\kappa$  and the minimum real part of the spectrum  $\min(\Re(\lambda_i))$  of the matrix associated with the discretisations on the grids  $\{g(0), \dots, g(3)\}$ . The results are shown in the Tables 4 and 5.

If we first consider the results in Table 4, we see that for the two radii of the embedded boundary, except for one situation, the discrete form (4.11), with  $\nu = 10$ , is positive definite. In case of grid  $g(3)$  with radius  $R = \sqrt{0.50}$ , we have that vanishing cut cells  $\Omega_e$  exist, which make the operator indefinite. Notice that even in this case the method yields good accuracy. Figure 9 shows the solution and the error of (4.11) for this situation.

Furthermore, between two grids we observe an average error reduction of a factor 12, which is suboptimal considering the optimal asymptotic factor 16. This suboptimal convergence behavior is natural and to be expected, since it is likely to arrive at grids with vanishing cut cells  $\Omega_e$  affecting the condition number of the discrete operator.

If we consider the results of (4.11, with  $\nu = 0$ , in Table 5), we see that in all cases the discrete operator is indefinite. Moreover, we see that the discretisation on mesh  $g(2)$  for the radius  $R = \sqrt{0.13}$  is less stable which is directly reflected in a sudden increase of the condition number  $\kappa$  and a small reduction of the error. Figure 10 shows the error of (4.11), for the cases  $\nu = 0$  and  $\nu = 10$ , on this  $g(2)$  grid with  $R = \sqrt{0.13}$ . We see clearly the stabilizing effect of the weight (4.6) in (4.11).

As an extra exposure, we solve with (4.11) and  $\mu = 10$  the BVP  $\Delta u = 0$ , with Dirichlet boundary conditions such that the solution is  $u = \arctan(\frac{x-1}{y})$ , on the domain as in Figure 7. To avoid the singularity at  $x = 1$ , we choose  $R = \sqrt{0.032} \approx 0.179$  for the circular embedded

	$R = \sqrt{0.13} \approx 0.361$		
	$\ u - u_h\ _{L^\infty(\Omega)}$	$\kappa$	$\min(\Re(\lambda_i))$
g(0)	2.9294e-003	2.7189e004	1.8183e-004
g(1)	3.3368e-004	2.2476e004	1.5288e-004
g(2)	1.4871e-005	8.0224e004	1.3117e-004
g(3)	3.7363e-006	2.8762e004	4.5802e-005
	$R = \sqrt{0.50} \approx 0.707$		
	$\ u - u_h\ _{L^\infty(\Omega)}$	$\kappa$	$\min(\Re(\lambda_i))$
g(0)	4.2920e-003	1.8397e004	1.6944e-004
g(1)	2.3569e-004	2.9286e004	1.2918e-004
g(2)	4.3262e-005	4.8409e004	9.5886e-005
g(3)	1.7262e-006	5.7696e005	-6.1279e-005

Table 4: The error of the approximation, the condition number and the minimum real part of the spectrum, of the fourth-order DG-discretisation (4.11), with  $\nu = 10$ , on grids as shown in Figure 7. The exact solution is  $u = \sin(x) \cos(y)$ .

boundary condition. The solution on the  $g(3)$  grid is shown in Figure 11. Table 6, shows the error  $\|u - u_h\|_{L^\infty(\Omega)}$ , the condition number  $\kappa$  and the minimum real part of the spectrum  $\min(\Re(\lambda_i))$ , of the DG-discretisation on the grids  $\{g(0), \dots, g(3)\}$ . We see that also for this radius of the embedded boundary, the discrete DG-form is stable on all grids  $\{g(0), \dots, g(3)\}$ .

#### 4.3 An embedded boundary for the convection term

Having studied the discretisation of the Poisson equation with an embedded boundary condition, and with the aim to solve a convection dominated singular perturbation problem in Section 4.4, we continue with the convection equation with an embedded boundary condition. So we consider on a domain  $\widehat{\Omega}$  the BVP

$$\mathbf{b} \cdot \nabla u = f \text{ in } \widehat{\Omega}, \quad u = u_0 \text{ on } \partial\Omega_{\text{in}}, \quad (4.12)$$

where  $\mathbf{b}$  is a constant vector denoting the direction of the convection. The boundary of the domain of interest  $\Omega$  is  $\partial\Omega = \partial\Omega_{\text{in}} \cup \partial\Omega_{\text{out}}$ , with the inflow boundary defined by  $\mathbf{b} \cdot \mathbf{n} < 0$  on  $\partial\Omega_{\text{in}}$  and the outflow boundary defined by  $\mathbf{b} \cdot \mathbf{n} > 0$  on  $\partial\Omega_{\text{out}}$ . We also split the boundary  $\partial\widehat{\Omega} = \partial\widehat{\Omega}_{\text{in}} \cup \partial\widehat{\Omega}_{\text{out}}$  of the whole domain  $\widehat{\Omega}$  in an upwind and a downwind boundary and now we consider the following weak formulation for the BVP (4.12) [9]: find  $u \in H^1(\widehat{\Omega})$  and  $p \in H^{1/2}(\partial\widehat{\Omega}_{\text{in}})$  such that

$$\begin{aligned} & - \int_{\widehat{\Omega}} \nabla v \cdot \mathbf{b} u \, dx + \int_{\partial\widehat{\Omega}_{\text{in}}} \mathbf{n} \cdot \mathbf{b} \, p v \, ds + \int_{\partial\widehat{\Omega}_{\text{out}}} \mathbf{n} \cdot \mathbf{b} \, u v \, ds + \int_{\partial\Omega_{\text{in}}} \mathbf{n} \cdot \mathbf{b} \, q u \, ds \\ &= \int_{\widehat{\Omega}} f v \, dx + \int_{\partial\Omega_{\text{in}}} \mathbf{n} \cdot \mathbf{b} \, q u_0 \, ds, \quad \forall v \in H^1(\widehat{\Omega}), \quad \forall q \in H^{1/2}(\partial\Omega_{\text{in}}), \end{aligned} \quad (4.13)$$

in which we assume that  $u$  on the fictitious domain  $\widetilde{\Omega}$  satisfies the differential equation and is continuation of the solution  $u$  on the domain  $\Omega$ . The solution of this problem is

	$R = \sqrt{0.13} \approx 0.361$		
	$\ u - u_h\ _{L^\infty(\Omega)}$	$\kappa$	$\min(\Re(\lambda_i))$
g(0)	4.4432e-003	6.5442e003	-2.4981e-004
g(1)	3.7480e-004	1.4921e004	-0.0195
g(2)	2.9433e-004	5.0569e005	-0.0027
g(3)	2.5061e-006	3.0911e004	-0.0570
	$R = \sqrt{0.50} \approx 0.707$		
	$\ u - u_h\ _{L^\infty(\Omega)}$	$\kappa$	$\min(\Re(\lambda_i))$
g(0)	1.3258e-002	1.7460e004	-0.0162
g(1)	1.0253e-003	2.6406e004	-9.1856e-004
g(2)	3.6020e-005	5.4214e004	-0.0684
g(3)	4.9052e-006	8.0311e005	-0.0770

Table 5: The error of the approximation, the condition number and the minimum real part of the spectrum, of the fourth order-order DG-discretisation (4.11), with  $\nu = 0$ , on grids as shown in Figure 7. The exact solution is  $u = \sin(x) \cos(y)$ .

	$R = \sqrt{0.032} \approx 0.179$		
	$\ u - u_h\ _{L^\infty(\Omega)}$	$\kappa$	$\min(\Re(\lambda_i))$
g(0)	3.6422e-001	2.6124e+004	2.7731e-004
g(1)	1.2682e-001	3.2321e+004	1.6839e-004
g(2)	5.8684e-002	2.2346e+004	1.5281e-004
g(3)	2.6119e-003	8.3446e+004	1.2924e-004

Table 6: The error of the approximation, the condition number and the minimum real part of the spectrum, of the fourth-order DG-discretisation (4.11), with  $\nu = 10$ , on grids as shown in Figure 7. The exact solution is  $u = \arctan(\frac{x-1}{y})$ .

straightforward because the boundary condition at  $\partial\Omega_{\text{in}}$  determines the solution along the corresponding characteristics.

As our first interest is an efficient fourth order discretisation of the convection diffusion equation on a domain as shown in Figure 7, we expect it to be highly improbable that instability will occur in the discrete operator of the DG formulation for the convection part in combination with the fourth order modified DG-formulation for the diffusion part (4.11). Hence we eliminate in (4.13) the Lagrange multiplier  $p$  with the value of  $u$  on  $\partial\hat{\Omega}_{\text{in}}$  and we take for the test functions  $q = v$  on the boundary  $\partial\hat{\Omega}_{\text{in}}$ , yielding the following formulation: find  $u \in H^1(\hat{\Omega})$  such that

$$\begin{aligned} & - \int_{\hat{\Omega}} \nabla v \cdot \mathbf{b} u \, dx + \oint_{\partial\hat{\Omega}} \mathbf{n} \cdot \mathbf{b} \, uv \, ds + \int_{\partial\Omega_{\text{in}}} \mathbf{n} \cdot \mathbf{b} \, vu \, ds \\ &= \int_{\hat{\Omega}} fv \, dx + \int_{\partial\Omega_{\text{in}}} \mathbf{n} \cdot \mathbf{b} \, vu_0 \, ds, \quad \forall v \in H^1(\hat{\Omega}). \end{aligned} \tag{4.14}$$

Next we introduce the DG-formulation for the convection equation (4.12) on partitionings

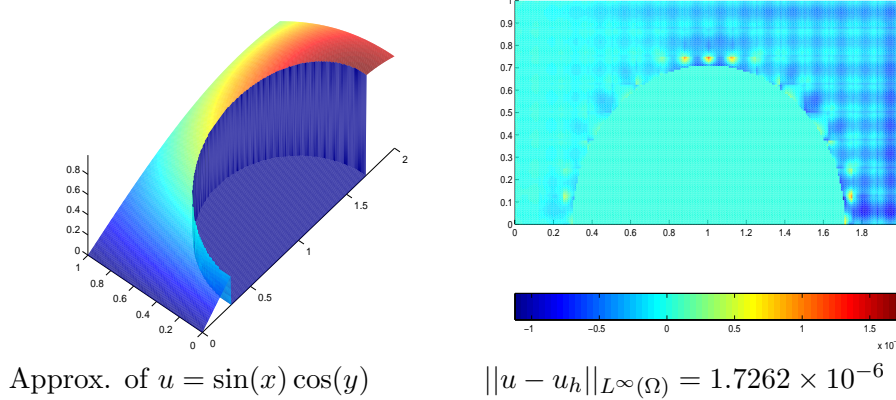


Figure 9: The solution and the error on the domain  $\Omega$  of the problem  $-\Delta u = 2 \sin(x) \cos(y)$  discretized by (4.11), where  $\nu = 10$ . The discretisation is made on grid  $g(3)$  as shown Figure 7. The radius of the circular embedded boundary is  $R = \sqrt{0.50}$ .

according to (2.3). For the embedded boundary parts we have to distinguish inflow boundary parts and outflow boundary parts. For the convection equation, outflow boundary parts can be neglected whereas the inflow parts provide the solution with a boundary condition. To show the technique used and its related DG discretisation, we consider the simple case of mesh  $g(0)$  in Figure 7 and we take constant  $\mathbf{b} = (1, 0)$  in (4.12). We find two cells  $\widehat{\Omega}_1$  and  $\widehat{\Omega}_2$  both with an interior circle segment  $\gamma_e$ . For the left cell  $\widehat{\Omega}_1$  the embedded boundary segment  $\gamma_1$  is an outflow boundary and, hence, can be neglected, while the embedded boundary  $\gamma_2$  in cell  $\widehat{\Omega}_2$  is an inflow boundary where we take into account the boundary condition. First we treat cell  $\widehat{\Omega}_1$  as a usual DG-cell for which we write the formulation: find  $u \in H^1(\widehat{\Omega}_1)$  such that

$$\begin{aligned} - \int_{\widehat{\Omega}_1} \nabla v \cdot \mathbf{b} u \, dx + \int_{\partial\widehat{\Omega}_1, \text{in}} (\mathbf{n} \cdot \mathbf{b} u_0) v \, ds + \int_{\partial\widehat{\Omega}_1, \text{out}} (\mathbf{n} \cdot \mathbf{b} u) v \, ds \\ = \int_{\widehat{\Omega}_1} f v \, dx, \quad \forall v \in H^1(\widehat{\Omega}_1). \end{aligned} \quad (4.15)$$

Next we use (4.14) for the cell  $\widehat{\Omega}_2$  in order to arrive at: find  $u \in H^1(\widehat{\Omega}_2)$  such that

$$\begin{aligned} - \int_{\widehat{\Omega}_2} \nabla v \cdot \mathbf{b} u \, dx + \oint_{\partial\widehat{\Omega}_2} \mathbf{n} \cdot \mathbf{b} uv \, ds + \int_{\gamma_2} \mathbf{n} \cdot \mathbf{b} vu \, ds + \int_{\Gamma_{\text{int}}} \mathbf{n} \cdot \mathbf{b} vu \, ds \\ = \int_{\widehat{\Omega}_2} f v \, dx + \int_{\gamma_2} \mathbf{n} \cdot \mathbf{b} vu_0 \, ds + \int_{\Gamma_{\text{int}}} \mathbf{n} \cdot \mathbf{b} vu^- \, ds, \quad \forall v \in H^1(\widehat{\Omega}_2), \end{aligned} \quad (4.16)$$

where  $u^- = u|_{\partial\Omega_1} = u|_{\Gamma_{\text{int}}}$  is the upwind value of  $u$  obtained from  $\widehat{\Omega}_1$ . And hence the weak formulation on the partitioning  $\widehat{\Omega}_h = \widehat{\Omega}_1 \cup \widehat{\Omega}_2$  is obtained by adding (4.15) and (4.16). The

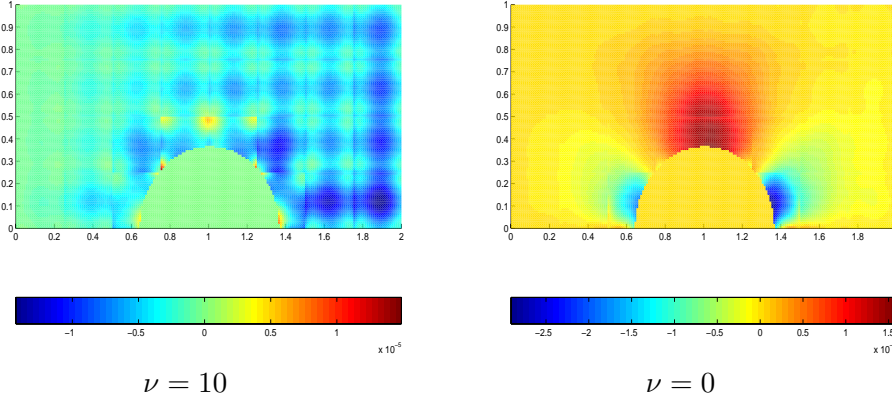


Figure 10:  $\|u - u_h\|_{L^\infty(\Omega)}$  of the problem  $-\Delta u = 2 \sin(x) \cos(y)$  with solution  $u = \sin(x) \cos(y)$  and circular embedded boundary on grid  $g(2)$  as in Figure 7, discretized by (4.11).

result is: find  $u \in H^1(\widehat{\Omega}_h)$  such that

$$\begin{aligned} & - \int_{\widehat{\Omega}} \nabla v \cdot \mathbf{b} u \, dx + \int_{\partial\widehat{\Omega}_{1,\text{in}}} (\mathbf{n} \cdot \mathbf{b} u_0) v \, ds + \int_{\partial\widehat{\Omega}_{1,\text{out}}} (\mathbf{n} \cdot \mathbf{b} u) v \, ds \\ & + \oint_{\partial\widehat{\Omega}_2} \mathbf{n} \cdot \mathbf{b} \, uv \, ds + \int_{\gamma_2} \mathbf{n} \cdot \mathbf{b} \, vu \, ds + \int_{\Gamma_{\text{int}}} \mathbf{n} \cdot \mathbf{b} \, v(u - u^-) \, ds \\ & = \int_{\widehat{\Omega}_2} fv \, dx + \int_{\gamma_2} \mathbf{n} \cdot \mathbf{b} \, vu_0 \, ds, \quad \forall v \in H^1(\widehat{\Omega}_h). \end{aligned} \quad (4.17)$$

Here,  $\Gamma_{\text{int}} = \partial\Omega_1 \cap \partial\Omega_2$  is the common interface on which the true solution is continuous. However, continuity is not required outside the domain  $\Omega$  and, hence, not on  $\widetilde{\Gamma}_{\text{int}} = \widehat{\Gamma}_{\text{int}} \cap \Omega$ .

To proceed, we consider the DG-formulation for the convection equation on finer partitionings. Cells  $\widehat{\Omega}_{e,+} \in \widehat{\Omega}_h$ , having either the embedded boundary segment  $\gamma_e$  as an outflow wall or do not have an embedded boundary at all, are denoted 'normal' DG-cells, while cells  $\widehat{\Omega}_{e,-} \in \widehat{\Omega}_h$  with the inflow embedded boundary segment  $\gamma_e$ , are treated by (4.16). And hence we arrive at: find  $u \in H^1(\widehat{\Omega}_h)$  such that

$$\begin{aligned} & \sum_{\widehat{\Omega}_{e,+} \in H^1(\widehat{\Omega})} \left[ - \int_{\widehat{\Omega}_{e,+}} \nabla v \cdot \mathbf{b} u \, dx + \int_{\partial\widehat{\Omega}_{e,+,\text{in}}} (\mathbf{n} \cdot \mathbf{b} u^-) v \, ds \right. \\ & \left. + \int_{\partial\widehat{\Omega}_{e,+,\text{out}}} (\mathbf{n} \cdot \mathbf{b} u) v \, ds \right] + \sum_{\widehat{\Omega}_{e,-} \in H^1(\widehat{\Omega})} \left[ - \int_{\widehat{\Omega}_{e,-}} \nabla v \cdot \mathbf{b} u \, dx \right. \\ & \left. + \oint_{\partial\widehat{\Omega}_{e,-}} \mathbf{n} \cdot \mathbf{b} \, uv \, ds + \int_{\gamma_e} \mathbf{n} \cdot \mathbf{b} \, vu \, ds \right] + \int_{\Gamma_{\text{int}}} \mathbf{n} \cdot \mathbf{b} \, v(u - u^-) \, ds \\ & = \sum_{\widehat{\Omega}_e \in \widehat{\Omega}_h} fv \, dx + \int_{\gamma_{\text{in}}} \mathbf{n} \cdot \mathbf{b} \, vu_0 \, ds, \quad \forall v \in H^1(\widehat{\Omega}_h), \end{aligned} \quad (4.18)$$

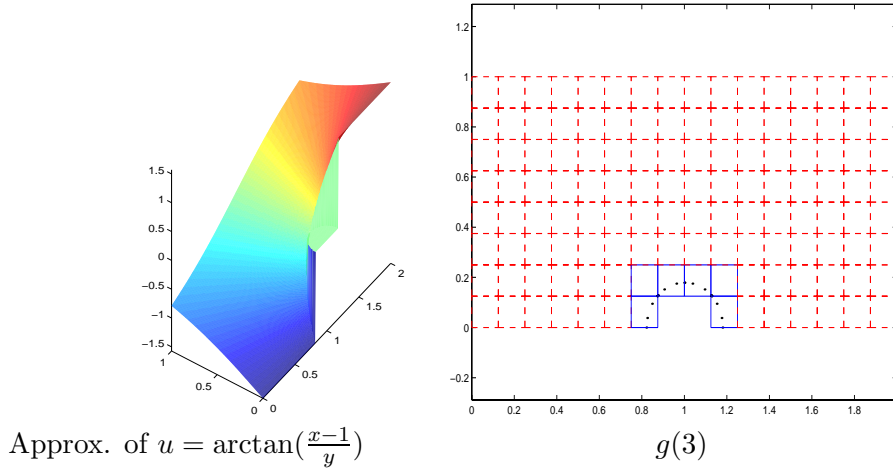


Figure 11: The solution on the domain  $\Omega$  of the problem  $-\Delta u = 0$  discretized by the fourth-order DG-discretisation (4.11), with  $\nu = 10$ . The discretisation is made on grid  $g(3)$ . The radius of the circular embedded boundary is  $R = \sqrt{0.032}$ .

where  $u^-|_{\partial\hat{\Omega}_{e,+,\text{in}} \cap \partial\Omega} = u_0$ . The discretisation of (4.18) in combination with (4.9) gives a discrete formulation of the convection diffusion equation

$$-\Delta u + \mathbf{b} \cdot \nabla u = f \quad \text{in } \hat{\Omega}, \quad u = u_0 \quad \text{on } \partial\Omega, \quad (4.19)$$

for domains with embedded Dirichlet boundary condition partitioned as, i.e., shown in Figure 7.

#### 4.4 Application to a convection diffusion problem with dominating convection on a domain with a curved embedded boundary

In this section we solve the following singularly perturbed convection diffusion problem (see Figure 12 and also Figure 7).

$$-\varepsilon\Delta u + u_x = f \quad \text{on } \hat{\Omega} = \{(x, y) \mid 0 < x < 2, 0 < y < 1\}, \quad (4.20)$$

$$u = 0 \quad \text{on } \Gamma_D = \{(x, y) \mid x = 0, 0 < y < 1; 0 < x < 2, y = 1\},$$

$$u = 1 \quad \text{on } \gamma = \{(x, y) \mid (x - 1)^2 + y^2 = R^2; (x, y) > 0; R < 1\}, \quad (4.21)$$

$$\mathbf{n} \cdot \varepsilon \nabla u = 0 \quad \text{on } \Gamma_N = \{(x, 0) \mid 0 < x < R, R < x < 2\} \cup \{(2, y) \mid 0 < y < 1\}.$$

The solution of this boundary value problem has a rather complex structure [7]. At the upwind part of the circle a boundary layer of thickness  $O(\varepsilon)$  develops, since the solution has to satisfy the Dirichlet boundary condition on the circle. Downwind of the circle, a shear layer of thickness  $O(\sqrt{\varepsilon})$  extends over the domain  $\Omega$ . The transition between the boundary layer and the shear layer is difficult to analyze.

It is interesting to see how well this complex structure is captured by means of a fourth order DG-discretisation.

The DG-discretisation of (4.20) is obtained by taking a linear combination of (4.9) and (4.18). We take for  $S(\hat{\Omega}_h) \subset H^1(\Omega_h)$ , the tensor product of polynomials of degree less than

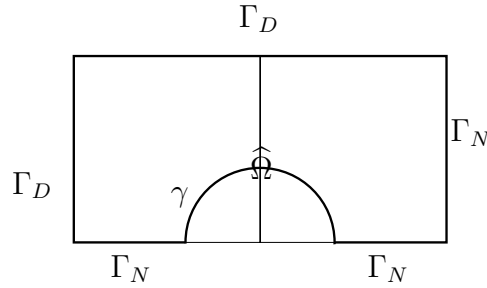


Figure 12: The domain for problem (4.20-4.21).

four in each of the coordinate directions. We construct a basis for  $S(\widehat{\Omega})$  from the cubics (3.13), defined on the unit interval, and a discretisation of problem (4.20) on meshes as shown in Figure 7 is obtained: find  $u_h \in S_h(\widehat{\Omega}_h)$  such that

$$\begin{aligned}
& \sum_{\widehat{\Omega}_e \in \widehat{\Omega}_h} (\varepsilon \nabla u_h, \nabla v_h)_{\widehat{\Omega}_e} - \langle \mathbf{n} \cdot \varepsilon \nabla u_h, v_h \rangle_{\Gamma_D} + \langle \mathbf{n} \cdot \varepsilon \nabla v_h, u_h \rangle_{\Gamma_D} - \\
& \quad \langle \langle \varepsilon \nabla u_h \rangle, [v_h] \rangle_{\widehat{\Gamma}_{int}} + \langle \langle \varepsilon \nabla v_h \rangle, [u_h] \rangle_{\Gamma_{int}} + \mu \langle \varepsilon \tilde{\gamma}_D(v_h), u_h \rangle_{\gamma} \\
& + \sum_{\widehat{\Omega}_{e,+} \in H^1(\widehat{\Omega})} \left[ - \int_{\widehat{\Omega}_{e,+}} \nabla v_h \cdot \mathbf{b} u_h \, dx + \int_{\partial \widehat{\Omega}_{e,+,\text{in}}} (\mathbf{n} \cdot \mathbf{b} u_h^-) v_h \, ds \right. \\
& \quad \left. + \int_{\partial \widehat{\Omega}_{e,+,\text{out}}} (\mathbf{n} \cdot \mathbf{b} u_h) v_h \, ds \right] + \sum_{\widehat{\Omega}_{e,-} \in H^1(\widehat{\Omega})} \left[ - \int_{\widehat{\Omega}_{e,-}} \nabla v_h \cdot \mathbf{b} u_h \, dx \right. \\
& \quad \left. + \oint_{\partial \widehat{\Omega}_{e,-}} \mathbf{n} \cdot \mathbf{b} u_h v_h \, ds + \int_{\gamma_e} \mathbf{n} \cdot \mathbf{b} v_h u_h \, ds \right] + \int_{\Gamma_{int}} \mathbf{n} \cdot \mathbf{b} v_h (u_h - u_h^-) \, ds \\
& = \mu \langle \varepsilon \tilde{\gamma}_D(v_h), 1 \rangle_{\gamma} + \int_{\gamma_{\text{in}}} \mathbf{n} \cdot \mathbf{b} v_h 1 \, ds, \quad \forall v_h \in S_h(\widehat{\Omega}_h).
\end{aligned} \tag{4.22}$$

Similar as for (4.11) the integrals over the internal and the embedded boundaries,  $\Gamma_{int}$  and  $\gamma_e$  are computed with a four-point Lobatto quadrature rule.

Figure 13 shows the solution of the discretisation of (4.22) on the  $g(3)$  grid as shown in Figure 7, for  $R = \sqrt{0.13}$  and  $\mu = 10/|\gamma_e|$ , for the different values of  $\varepsilon = 0.5, 0.25, 0.1$  and  $0.05$ . In all cases, we see clearly a boundary layer at the upwind side of the circle and the shear layer at the downwind side in the domain  $\Omega$ . The approximations for  $\varepsilon$  to 0.1 perfectly satisfy the boundary conditions on  $\partial\Omega$ . For values of  $\varepsilon \ll 1$ , the boundary layer is too sharp, to accurately be represented by piece-wise cubics on the grid  $g(3)$ . However, Figure 14 shows a side- and top-view of the solution for  $\varepsilon = 0.05$  on the finer mesh  $g(4)$ . The boundary layer is accurately captured and we see clearly the parabolic structure of the boundary layer and the shear layer [7].

In either case, these results show that DG-discretisations on regular rectangular meshes with an embedded boundary condition is effective.

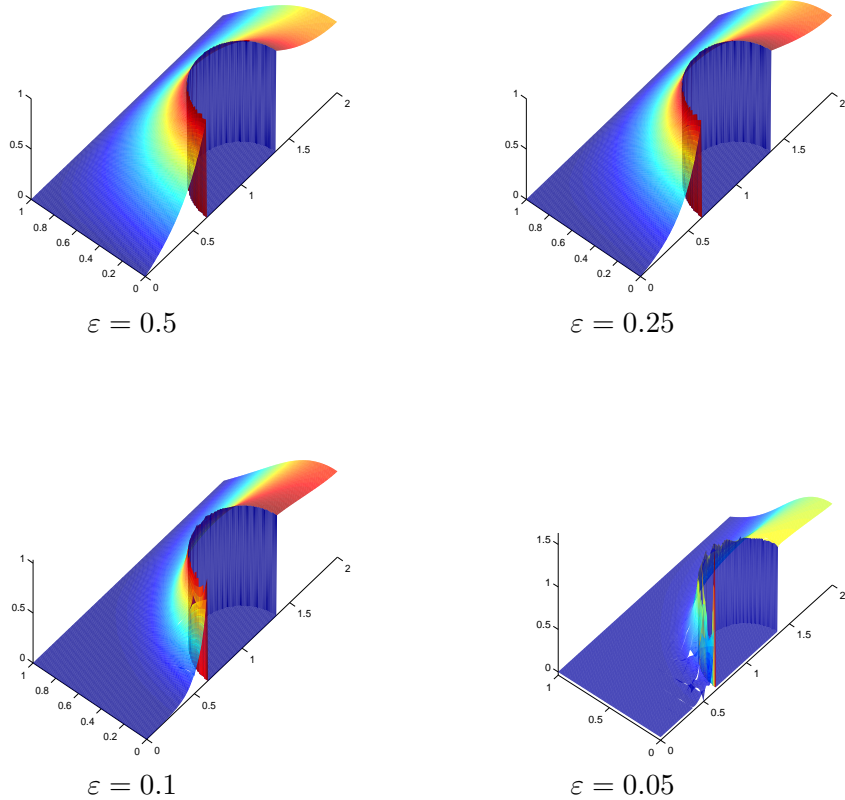


Figure 13: The approximate solution  $u_h$  of  $-\varepsilon \Delta u + u_x = 0$ , on the domain exterior of the circle, on mesh  $g(3)$  as shown in Figure 7, for the fourth-order DG discretisation with Dirichlet boundary condition  $u_0 = 1$  on the circle ( $R = \sqrt{0.13}$ ).

## 5. CONCLUSION

In this paper we propose a discontinuous Galerkin discretisation technique for solving 2-D second order elliptic PDEs on a structured regular rectangular grid, while the boundary value problem has a curved Dirichlet boundary.

We introduce two general weak formulations for the embedded boundary condition: the Lagrange multiplier form and the hybrid form. We discuss the stability of both formulations. We show by a numerical example that for the Lagrange multiplier formulation there exist locations of the embedded boundary condition for which the resulting linear system becomes singular, while this is not the case for the hybrid form. We observe that this (in)stability is directly linked with the test and trial space in the corresponding equivalent weak formulation of the problem with strongly imposed boundary conditions.

From either the hybrid or the Lagrange formulation we derive the family of discontinuous Galerkin methods for an embedded boundary condition. In general, these methods are unstable in the sense that there exist locations of the embedded boundary for which the resulting

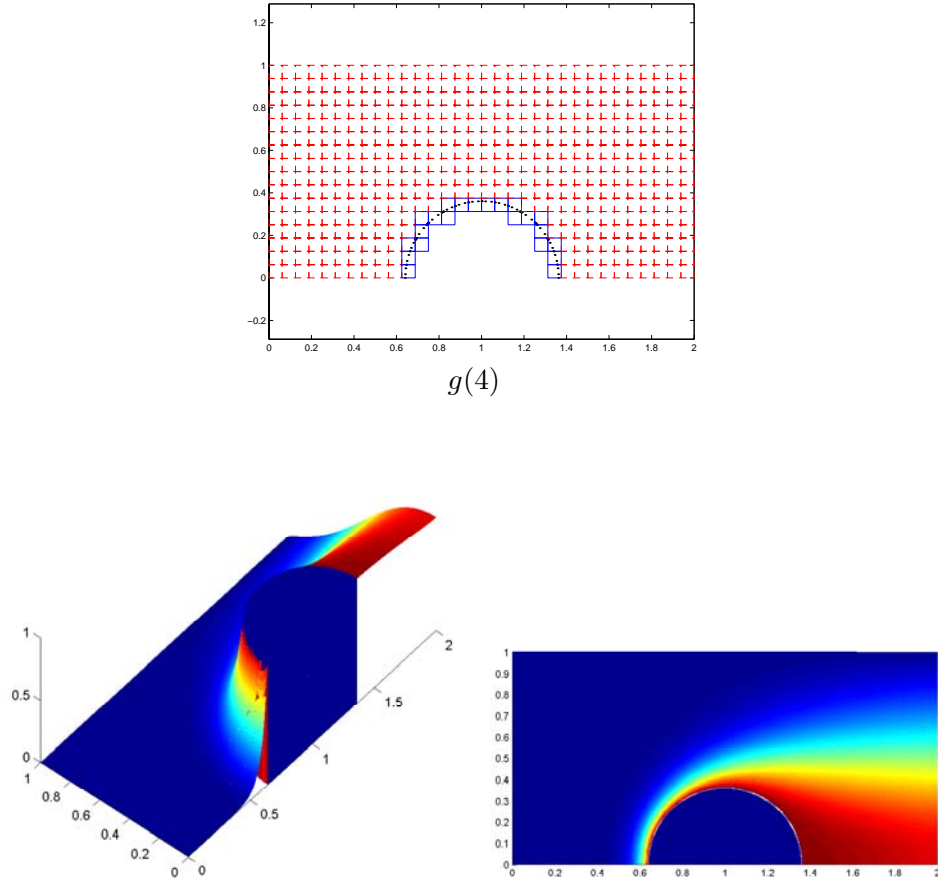


Figure 14: Side- and top-view of the approximate solution  $u_h$  of  $-0.05\Delta u + u_x = 0$ , on the domain exterior of the circle, on mesh  $g(4)$  as shown, for the fourth-order DG discretisation with Dirichlet boundary condition  $u_0 = 1$  on the circle ( $R = \sqrt{0.13}$ ).

linear system becomes singular. However, this instability is easily repaired. Considering the asymmetric Baumann-Oden variant for the embedded boundary, we only have to weight the embedded boundary with the traces of linear polynomials, to stabilize the method. We prove that adapted in this way, the DG-method is stable for the discretisation of the 1-D Poisson equation on a single cell with embedded boundary condition and we show that the method is positive definite. We further conclude that also the discrete operator of the discretisation of an adapted DG cell in combination with normal Baumann-Oden DG cells is positive definite.

On coarse and finer regular rectangular grids we solve the 2-D Poisson equation with a circular embedded boundary condition, approximated by cubic polynomials. We show that the DG-formulation for the embedded boundary is fourth order consistent both on the interior and on the boundary. By experiments, we show that on halving the grid size an average error reduction of a factor 12 can be expected, if an extra weight is introduced, weighting the embedded boundary with the trace of a linear polynomial. Moreover the corresponding linear systems are positive definite.

As an example we solve the Poisson equation with the singular solution,  $u = \arctan(x-1)/y$ ,

with a small embedded Dirichlet boundary condition around the point  $(1, 0)$ , to give an illustration of the discretisation technique used for the embedded boundary condition.

To further show the possibilities of the DG-discretisation, we solve a convection dominated boundary value problem with a circular embedded boundary condition. The solution of this problem shows a sharp boundary layer with a complex structure. The boundary layer is captured accurately by means of piece-wise cubic polynomials. Summarizing, we show that the proposed treatment of curved Dirichlet boundary conditions on a regular rectangular grid can be effective.

## REFERENCES

1. D.N. Arnold, F. Brezzi, B. Cockburn, and D. Marini. Unified analysis of discontinuous Galerkin methods for elliptic problems. *SIAM J Numer. Anal.*, pages 1749 – 1779, 2002.
2. Jean-Pierre Aubin. *Pure & applied mathematics*. John Wiley & sons, 1979.
3. I. Babuska, J. T. Oden, and J. K. Lee. Mixed-hybrid finite element approximations of second-order elliptic boundary-value problems. *Comp. Meth. in Appl. Mech. and Eng.*, 11:175–206, 1977.
4. C. E. Baumann and J. T. Oden. An  $hp$ -adaptive Discontinuous finite element method for computational fluid dynamics. *The university of Texas at Austin*, 1997.
5. C.E. Baumann. *An hp-adaptive discontinuous finite element method for computational fluid dynamics*. PhD thesis, The University of Texas at Austin, 1997.
6. R. Cortez and M. Minion. The Blob projection method for immersed boundary problems. *Journal of Computational Physics*, 161:428–453, 2000.
7. P. W. Hemker. A singularly perturbed model problem for numerical computation. *Journal of Comp. and Appl. Math.*, 76:277–285, 1997.
8. P.W. Hemker, W. Hoffmann, and M.H. van Raalte. Two-level Fourier analysis of a multigrid approach for discontinuous Galerkin discretisation. Technical Report MAS-R0206, CWI, Amsterdam, April 2002. to appear in SIAM SISC.
9. P.W. Hemker, W. Hoffmann, and M.H. van Raalte. Discontinuous Galerkin discretisation with embedded boundary conditions. *Computational Methods in Applied Mathematics*, 3:135–158, 2003.
10. P.W. Hemker and M.H. van Raalte. Fourier two-level analysis for higher dimensional discontinuous Galerkin discretisation. Technical Report MAS-R0227, CWI, Amsterdam, November 2002. to appear in Computing and Visualization in Science.
11. D.W. Hewett and C.S. Kueny. The dielectric boundary condition for the embedded curved boundary (ECB) method. Technical Report UCRL-JC-129703, Lawrence Livermore Nat. Lab., 1998. presented at the 16th International Conference on the Numerical Simulation of Plasmas, February 1998, Santa Barbara, CA.
12. P. Houston, C. Schwab, and E. Süli. Discontinuous  $hp$ -finite element methods for advection-diffusion problems. Technical Report No. 2000-07, ETHZ, Zürich, Switzerland, 2000.
13. C.S. Kueny. Embedded curved boundaries and adaptive mesh refinement. Technical Report UCRL-JC-129729, Lawrence Livermore Nat. Lab., 1998.
14. J. Nitsche. Über ein Variationsprinzip zur Lösung von Dirichlet Problemen bei Verwendung von Teilräumen die keinen Randbedingungen unterworfen sind. *Abh. Math. Sem. Univ. Hamburg*, 36:9, 1971.
15. J. T. Oden and G. F. Carey. Texas finite elements series. *Mathematical Aspects*, IV, Prentice-Hall, 1983.
16. J.T. Oden, I. Babuška, and C.E. Baumann. A discontinuous  $hp$  finite element method for diffusion problems. *J. Comp. Phys.*, 146:491–519, 1998.

17. C.S. Peskin. Numerical analysis of blood flow in the heart. *J. Comp. Phys.*, 25:220 – 252, 1977.
18. S. Prudhomme, F. Pascal, J.T. Oden, and A.Romkes. Review of a Priori Error Estimations for discontinuous Galerkin Methods. *TICAM report 00-27*, 2000.
19. J. F. Remacle, J. E. Flaherty, and M. S. Shephard. An Adaptive Discontinuous Galerkin Technique with an orthogonal basis applied to compressible flow problems. *SIAM Review vol 45, No. 1.*, pages 53 – 72, 2003.
20. E. Süli, C. Schwab, and P. Houston. *hp-DGFEM* for partial differential equations with non-negative characteristic form. In B. Cockburn, G. E. Karniadakis, and C.-W. Shu, editors, *Discontinuous Galerkin Methods. Theory, Computation and Applications*, volume 11 of *Lecture Notes in Comput. Sci. Engrg.*, pages 221–230. Springer-Verlag, New York, 2000.
21. C. Tu and C. S. Peskin. Stability and instability in the computation of flows with moving immersed boundaries: A comparison of three methods. *SIAM Journal on Scientific and Statistical Computing*, 13:1361–1376, 1992.